

The Technoarete Transactions on Recent Advances in Cyber security and Digital Forensics Journal

Volume No. 13

Issue No. 3

September - December 2024



ENRICHED PUBLICATIONS PVT.LTD

**JE - 18,Gupta Colony, Khirki Extn,
Malviya Nagar, New Delhi - 110017.**

E- Mail: info@enrichedpublication.com

Phone :- +91-8877340707

The Technoarete Transactions on Recent Advances in Cyber security and Digital Forensics Journal

Managing Editor

Mr. Amit Prasad

The Technoarete Transactions on Recent Advances in Cyber security and Digital Forensics Journal

(Volume No. 13, Issue No. 3, September - December 2024)

Contents

Sr. No	Article/ Authors	Pg No
01	A Bayesian Network Based Classification of Breast Lesion in Digital Mammogram <i>- Amruta V. Shelke</i>	97 - 104
02	Pipelined Implementation of CORDIC and 64-Point FFT with Memory Interfacing Module <i>- K. Naga Chaitanya, Dr. P. Trinatha Rao</i>	105 - 114
03	Supervised Learning Approach for Performance Evaluation of Digital Fundus Image Quality <i>- TP. Syed Ali Fathima Aasia, K. Gokulakrishnan, J. Jesu Vedha Nayahi</i>	115 - 128
04	Digital Wallets: A Detailed Study <i>- Akshat Kudesia, Dr. Jyoti Pradhan</i>	129 - 136
05	Alternating Direction Method-Analysis Based Approach for Image in Painting <i>- B. H. Deokate, P.M.Patil, P. B. Lonkar</i>	137 - 149

A Bayesian Network Based Classification of Breast Lesion in Digital Mammogram

Amruta V. Shelke

Savitribai Phule Pune University,
Maharashtra, India

ABSTRACT

Breast cancer is a serious issue in the worldwide females. Breast cancer is the type of cancer which develops from breast cells. For detection of breast cancer there are different types of screening techniques are available. For detection of breast cancer this paper includes several techniques. In this paper, the first step was to remove noise from the image; median filter is used to remove the unwanted noise in the image. In the MIAS database pectoral muscles are available in the image, pectoral muscle are removed by calculating the thresholding value of an image. The entropy based segmentation approach is proposed to segment a gray-scale breast image. The approach calculates the histogram of an image also finds the entropy value of image. Then by finding the thresholding value of an image the segmented image is shown at the output. In this paper, an efficient and fast entropic method for noisy cell image segmentation is presented. Then the features like mean, standard deviation, Entropy, Skewness, Kurtosis, Variance, Energy, Correlation, Smoothness and Root mean square are extracted from a segmented image, this features are then given to the input of Bayesian network to classify the image according to the feature value. Experimental results show that the proposed method is efficient and much more tolerant to noise than other techniques.

Keywords: Entropy, Breast cancer, Bayesian network, median filter, pectoral muscle, noise, ROI

1. INTRODUCTION

Breast cancer is the most common breast cancer in the worldwide females. The Breast cancer is a type of cancer that develops from breast cells. Around 18.2% of all cancer deaths worldwide, including both males and females, are from breast cancer. Breast cancer is the serious matter in developed nations comparing to developing ones. There are some reasons behind this breast cancer that is more common in elderly women, women in the richest countries live much longer than those in the poorest nations. Because of different lifestyle and eating habits of females in rich and poor countries is also a contributory factor. According to the National Cancer Institute, 232,380 female breast cancers and 2,240 male breast cancers are reported in the USA each year. According to the World Health Organisation (WHO), seven lakh Indians die of cancer every year, while over 10 lakh are newly diagnosed with some form of the disease.

The origin of breast cancer is from the inner lining of milk ducts or the lobules that supply them with milk. Malignant tumor spread to other parts of the body. The breast cancer that starts off in the lobules is known as lobular carcinoma, while one that developed from the ducts is called ductal carcinoma.

There are billions of microscopic cells available in the body. The cancer cells multiply in orderly fashion; new cells are made to replace the ones that died.

The majority of breast cancer occurs in females. The invasive breast cancer is spread over the body part such as bones, liver or lungs and the non-invasive breast cancer is still inside its place of origin and has not broken out. In cancer, the cells multiply uncontrollably and there are too many cells, progressively more and more than there should be. However, it is difficult for radiologists to provide accurate and uniform evaluation for the mammograms generated. The advances of digital image processing radiologists have an opportunity to improve their diagnosis with the aid of computer system.

In this paper the median filter is used to remove noise in the image. Filtering is the technique for modifying or enhancing an image. After removing noise from the image the pectoral muscles are removed from the image. The entropy segmentation is used to detect ROI which is present in the image. The features are extracted from the ROI part of image and then given to the classifier to classify the image is normal or abnormal. The paper is organized as follows: Section 2 presents the flow of the method, preprocessing phase, segmentation, feature extraction and classifier. Section 3 shows the implementation and result.

2. MATERIALS AND METHODS

2.1 Preprocessing

The main goal of the preprocessing is to improve the image quality to make it ready to further processing by removing or reducing the unrelated and surplus parts in the background of the mammogram image. Mammograms are medical images that are complicated to interpret. To remove the noise and unwanted data, a median filter is used. Median filter preserves edges while removing noise. Image processing operations implemented with filtering include smoothing, sharpening, and edge enhancement. In image processing, filters are mainly used to suppress either the high frequencies in the image, i.e. smoothing the image, or the low frequencies, i.e. enhancing or detecting edges in the image. Filtering is a neighborhood operation, in which the value of any given pixel in the output image is determined by applying some algorithm to the values of the pixels in the neighborhood of the corresponding input pixel. The median filter is a sliding-window spatial filter. It replaces the value of the center pixel with the median of the intensity values in the neighborhood of that pixel. A median filter is more effective than convolution when the goal is to simultaneously reduce noise and preserve edges.

Pectoral muscle removal operation is important in medio- lateral oblique view (MLO), where the pectoral muscle, slightly brighter compared to the rest of the breast tissue, can appear in the mammogram. In properly imaged MLO mam- mograms, the pectoral muscle is visible as a triangular region of high-density at the upper posterior part of the image. Tex- ture of the pectoral muscle may also be similar to some ab- normalities and may cause false positives in the detection of suspicious masses. Pectoral muscles are the regions in mam- mograms that contain brightest pixels. These regions must be removed before detecting the tumor cells so that mass detec- tion can be done efficiently.

2.2 Segmentation

Segmentation is the process of partitioning a digital image into multiple regions. For this purpose the entropy segmenta- tion is used to segment the image. The following diagram shows the flow of entropy segmentation.

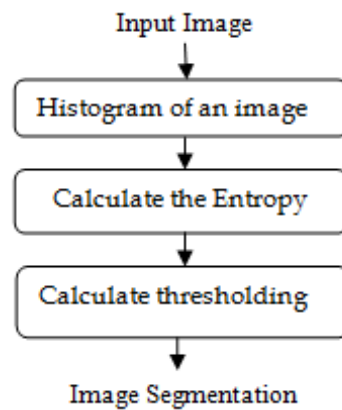


Figure 1: Segmentation algorithm

Histograms show the distribution of data values across a data range. They do this by dividing the data range into a certain number of intervals, tabulating the number of values that fall into each interval and plotting the values in the bins using bars or wedges of varying height. Entropy is a concept of information theory. It is used to measure the amount of in- formation. It is defined in terms of the probabilistic behavior of a source of information. Entropy can best represent the information containing in the image. The approach of image segmentation based on entropy algorithm is used to segment foreground and background image. Suppose $p=\{p_1,p_2,,,p_n\}$ be a finite discrete pro-bability distribution that satisfies these conditions

$$p(t) \geq 0, \text{ where } t=0,1,2...n$$

The amount of uncertainty of the distribution, is called the entropy of the distribution, P. The Shannon entropy of the distribution, P, a measure of uncertainty and denoted by $E(P)$, is defined as

$$E(P) = - \sum_{t=1}^n P_t \log_2 P_t \quad (1)$$

Additive entropy is

$$E(E1+E2)=E1(t)+E2(t) \quad (2)$$

Segmentation involves separating an image into regions (or their contours) corresponding to objects[1]. Usually try to segment regions by identifying common properties. Or, similarly, we identify contours by identifying difference between regions (edges).

The simplest property that pixels in a region can share is intensity. So, a natural way to segment such regions is through thresholding, the separation of light and dark regions. Thresholding creates binary images from grey-level ones by turning all pixels below some threshold to zero and all pixels above that threshold to one.

Thresholding method in image segmentation that yields all the pixels and assumes the algorithm in two cases i.e. darkness and brightness.

2.3 Feature Extraction

After the segmentation part, the features are extracted from the segmented images which are used for the classification. Then by extracting the feature from segmented image the classifier gives output normal or abnormal image. There are various features like mean, standard deviation, Entropy, Skewness, Kurtosis, Variance, Energy, Correlation, Smoothness, and Root Mean Square. These features are calculated by following formulas: There are various features like mean, standard deviation, Entropy, Skewness, Kurtosis, Variance, Energy, Correlation, Smoothness and Root mean square (rms). These features are calculated by following formulas:

Mean-

The mean, μ of the pixel values in the defined window, estimates the value in the image in which central clustering occurs. The mean can be calculated using the formula:

$$\mu = \frac{1}{MN} \sum_{i=1}^M \sum_{j=1}^N p(i, j) \quad (3)$$

Where $p(i,j)$ is the pixel value at point (i,j) of an image of size $M \times N$.

Standard deviation-

The Standard Deviation, σ is the estimate of the mean square deviation of grey pixel value $p(i, j)$ from its mean value m . Standard deviation describes the dispersion within a local region

$$\sigma = \sqrt{\frac{1}{MN} \sum_{i=1}^M \sum_{j=1}^N (p(i, j) - \mu)^2} \quad (4)$$

Entropy-

Entropy, h can also be used to describe the distribution variation in a region. Overall entropy of the image can be calculated as:

Entropy is defined as

$$h = - \sum_{k=0}^{L-1} Pr_k (\log Pr_k) \quad (5)$$

Where, Pr_k is the probability of the k^{th} grey level, which can be calculated as $Z_k / (M * N)$, Z_k is the total number of pixels with the k^{th} grey level and L is the total number of grey levels.

Skewness-

Skewness, S characterizes the degree of asymmetry of a pixel distribution in the specified window around its mean. Skewness is a pure number that characterizes only the shape of the distribution. The formula for finding Skewness is given in the below equation:

$$s = \frac{1}{MN} \sum_{i=1}^M \sum_{j=1}^N \left(\frac{g(i,j) - \mu}{\sigma} \right)^3 \quad (6)$$

Kurtosis-

Kurtosis, K measures the Peakness or flatness of a distribution relative to a normal distribution. The conventional definition of kurtosis is:

$$K = \frac{1}{MN} \sum_{i=1}^M \sum_{j=1}^N \left(\frac{g(i,j) - \mu}{\sigma} \right)^4 - 3 \quad (7)$$

Variance-

Variance is the square root of standard deviation or it is the average of the squared differences from the Mean.

$$\text{variance} = \sqrt{SD} \quad (8)$$

Energy-

Energy returns the sum of squared elements in the Grey Level Co-Occurrence Matrix (GLCM). Energy is also known as uniformity. The range of energy is $[0, 1]$.

Mathematical equation,

$$E = \sum_i \sum_j g(i,j)^2 \quad (9)$$

Correlation-

Correlation returns a measure of how correlated a pixel is to its neighbor over the whole image. The range of correlation is $[-1, 1]$. Correlation is 1 or -1 for a perfectly positively or negatively correlated

image. Correlation is NaN (Not a Number) for a constant image. The below equation shows the calculation of Correlation. Evaluates how a pixel is related to its neighbor.

$$correlation = \sum_{i,j} \frac{(i - \mu_i)(j - \mu_j) P(i, j)}{\sigma_i \sigma_j} \quad (10)$$

Smoothness-

Relative smoothness, R is a measure of grey level contrast that can be used to establish descriptors of relative smoothness. The smoothness is determined using the formula:

$$R = 1 - \frac{1}{1 + \sigma^2} \quad (11)$$

Root Mean Square-

The RMS (Root Mean Square) computes the RMS value of each row or column of the input, along vectors of a specified dimension of the input, or of the entire input. The RMS value of the j^{th} column of an M-by-N input matrix u is given by below equation:

$$y = \sqrt{\frac{\sum_{i=1}^M |u_{ij}|^2}{M}} \quad (12)$$

2.4 Bayesian Network

Bayesian networks are a statistical method for Data Mining, a statistical method for discovering valid, novel and potentially useful patterns in data. Bayesian networks are used to represent essential information in databases in a network structure. The network consists of edges and vertices, where the vertices are events and the edges relations between events. The networks can be used to represent domain knowledge, and it is possible to control inference[11]. A simple usage of Bayesian networks is denoted naive Bayesian classification.

$$p(x_1, \dots, x_n) = \prod_{i=1}^n P(x_i | c_j) \quad (13)$$

The aim of supervised classification is to classify instances i given by certain characteristics $x_i = \{x_{i1}, \dots, x_{in}\}$ into r class labels, c_i , $i=1, \dots, r$. x_{il} denotes the value of variable x_l observed in instance i . The main principle of a Bayesian classifier is the application of Bayes' theorem.

3. EXPERIMENTAL RESULT

In this section, the results of the proposed approach are presented. First the preprocessing is done by the median filter and also pectoral muscles are removed. Then this image is segmented by using the entropy segmentation method, features are extracted from segmented image and the output result is shown with the help of Bayesian network. The Bayesian network shows the image is abnormal image.

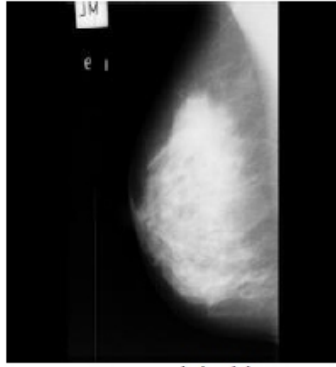


Figure 2: Original image

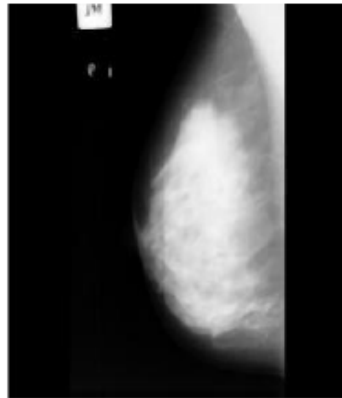


Figure 3: Filtered image



Figure 4: Pectoral muscles detected

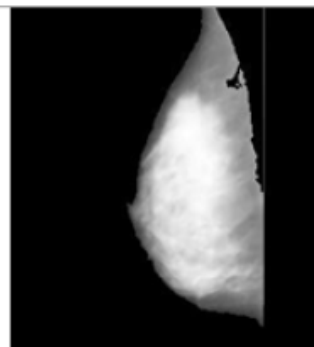


Figure 5: Image after removing pectoral muscle

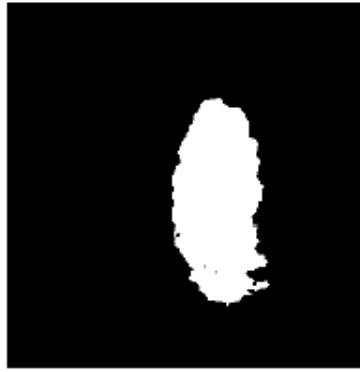


Figure 6: Segmented image

4. CONCLUSION

Although In this study, an automatic diagnosis system to detect the breast cancer by using Bayesian neural network is presented. In this study by using several preprocessing techniques the unwanted part is removed in the image. Using Entropy segmentation it shows the tumor area in the image. Then the Bayesian classifier is used to show the image result on the basis of features that are extracted from the image. The accuracy of this method is high up to certain extent for the MIAS database. The results of this method can be improved by taking the combination of Bayesian network with another classifier.

5. REFERENCES

- [1] R. Ramani, Dr. N.Suthanthira Vanitha, S. Valarmathy. "The Pre-Processing Techniques for Breast Cancer Detection in Mammography Images", *I.J. Image, Graphics and Signal Processing*, 2013, 5, pp- 47-54.
- [2] R. C. Gonzalez. "Digital Image processing using Mat- lab" Pearson publication, 2005.
- [3] H. Abdellatif, t. E. Taha, o. F. Zahran, w. Al-naumy, f. E. Abdel-samie, "k9. Automatic segmentation of digital mammograms to detect masses," *30th national radio science conference*, 2013, pp-557-565.
- [4] R. Subash Chandra Boss, K. Thangavel, D. Arul Pon Daniel, "Automatic Mammogram image Breast Region Extraction and Removal of Pectoral Muscle".
- [5] Chengxin Yan a, Nong Sang a, Tianxu Zhang, "Local entropy-based transition region extraction and threshold- ing," *Pattern Recognition Letters*, 24 (2003), pp 2935– 2941.
- [6] Amar Partap Singh Pharwaha, Baljit Singh, "Shannon and Non-Shannon Measures of Entropy for Statistical Texture Feature Extraction in Digitized Mammograms *Proceedings of the World Congress on Engineering and Computer Science 2009 Vol II*, October 20-22, 2009, ISBN: 978-988-18210-2-7.
- [7] Samy Sadek, Sayed Abdel-Khalek "Generalized α - Entropy Based Medical Image Segmentation" *Journal of Software Engineering and Applications*, 2014, 7, pp- 62- 67.
- [8] Pradeep N., Girisha H., Sreepathi B. And Karibasappa K. "feature extraction of mammograms", *international jour- nal of bioinformatics research*, volume 4, issue 1, 2012, pp.-241 -244.
- [9] W.R. Silva, D. Menotti, arwaha, "Classification of Mammograms by the Breast Composition," *The 2012 International Conference on Image Processing, Computer Vision, and Pattern Recognition*.
- [10] Amir Fallahi, Shahram Jafari, "An Expert System for Detection of Breast Cancer Using Data Preprocessing and Bayesian Network," *International Journal of Ad- vanced Science and Technology*, Vol. 34, September, 2011, pp 65-70.
- [11] S.Kharyal, S.Agrawal2, S. Soni, "Using Bayesian Belief Networks for Prognosis & Diagnosis of Breast Cancer", *International Journal of Advanced Research in Computer and Communication Engineering*, Vol. 3, Issue 2, Febru- ary 2014, pp-5423-5427.
- [12] Alok Sharma and Kuldip K. Paliwal, "A Gene Selection Algorithm using Bayesian Classification Approach", *American Journal of Applied Sciences*, 9 (1), pp- 127- 131

Pipelined Implementation of CORDIC and 64-Point FFT with Memory Interfacing Module

K. Naga Chaitanya¹, Dr. P. Trinatha Rao²

¹M.Tech VLSI, Department of ECE, GITAM University Hyderabad GITAM University, Hyderabad, India

²Associate.Professor, Department of ECE, GITAM University Hyderabad GITAM University, Hyderabad, India

ABSTRACT

Signal processing plays an important role in the field of communication Engineering. The amount of data that is received is processed by using different algorithms. Discrete Fourier Transform (DFT) is one of the technique that is used to compute the data. Direct computation of DFT results in complexity; as a result Fast Fourier Transform (FFT) is one of the algorithms to reduce the complexity. The proposed paper presents the parallel-pipelined implementation of radix-2 fixed point 32-point FFT algorithm using state machine as controller and fixed point pipelined implementation of Linear CORDIC that operates for the angles $-\frac{\pi}{2} \leq \theta \leq \frac{\pi}{2}$. of 64-point FFT are obtained in $M = \log_2 N$ clock cycles due to multi processor technique. Initially FFT functionality is checked using MATLAB and finally simulated and synthesized using Xilinx ISE 14.1. Besides CORDIC algorithm is implemented in both MATLAB and in Xilinx on Virtex-7. The main objective of this work is to obtain an area efficient FFT and CORDIC without performance loss that could be used as a part of Signal processing.

Keywords: Signal processing, DFT, FFT, CORDIC, state machine controller

1. INTRODUCTION

A signal in communication systems is referred as a function that conveys information about the behavior or attributes about information contained in the signals, signal processing is done on the signals. As the signals produced from physical quantities are analog in nature, these signals are converted in to discrete by sampling technique before processing. Therefore Discrete Time Signal processing is for sampled signals, defined only at discrete points in time and as such are quantized in time, but not in magnitude. In Digital Signal Processing (DSP) working on frequency domain is advantageous when compared to time domain [1]. This is overcome by Discrete Fourier Transform (DFT) that converts a signal in discrete time domain to discrete frequency domain. Computation of DFT is performing various mathematical operations like addition, multiplication etc on the received data. Computation directly by using DFT algorithm is quite tedious and complex which influences in global computation cost of design that consumes N^2 additions and $N(N - 1)$ multiplications. Cooley and Turkey developed the well-known radix-2 FFT algorithm to reduce the computational load of the DFT [2].

The paper is organized into five sections. In section-III we discuss the brief view of FFT, in section-IV about CORDIC algorithm and finally section-V gives the opted methodology and in VI Simulation results of CORDIC and FFT.

2. LITERATURE REVIEW

Brett W. Dickson and Albert A. Conti proposed a Pipelined Fast Fourier Transform (FFT) architectures, which are efficient for long instances (32k points and greater), are critical for modern digital communication and Radar systems. For long instances, Single-Path Delay- Feedback (SDF) FFT architectures minimize required memory, which can dominate circuit area and power dissipation. Their paper presents a parallel Radix-22 SDF architecture capable of significantly increased pipelined throughput at no cost to required memory or operating frequency. A corresponding parallel coefficient generator is also presented. Resource utilization results and analysis are presented targeted for a 45nm silicon-on-insulator (SOI) application-specific integrated circuit (ASIC) process. Multipliers implemented using Vedic mathematics is superior in terms of area efficiency. Carry Select Adders (CSLA) are one of the fastest adders used in several processors to perform fast and complex arithmetic functions. In the proposed paper, the Vedic multiplier which is developed using the Urdhva Tiryakbayam Sutra along with modified carry select adder is used to perform a Radix-22 pipeline Fast Fourier Transform. The Fast Fourier Transform (FFT) which is implemented using Vedic multiplier and adder is then compared with FFT implemented using traditional multipliers and adders and its performance is verified.

3. FAST FOURIER TRANSFORM ALGORITHM

Fast Fourier Transform (FFT) is a commonly used technique for the computation of Discrete Fourier Transform (DFT) [3]. DFT computations are required in the fields like filtering, spectral analysis, video processing etc. to calculate the frequency spectrum or to identify a system's frequency response from its impulse response and vice versa. Based on how one divides a set of N inputs into two sets of N/2 numbers, there are two types of radix-2 FFT algorithm or Cooley-Turkey algorithm. They are [4]

- i. Decimation in time FFT (DIT-FFT)
- ii. Decimation in frequency FFT (DIF-FFT).

In the proposed paper implementation of FFT algorithm is done using DIT-FFT.

The N-point discrete Fourier transform is defined by

$$X_n = \sum_{k=0}^{N-1} x_k W^{nk} \quad (1)$$

$$X_n = \sum_{k=0}^{\frac{N}{2}-1} x_{2k} W^{2nk} + \sum_{k=0}^{\frac{N}{2}-1} x_{2k+1} W^{(2n+1)k} \quad (2)$$

Therefore

$$X_n = \sum_{k=0}^{N/2-1} x_{2n} W_N^{nk} + W_N^{nk} \sum_{k=0}^{N/2-1} x_{2n+1} W_N^{nk} \quad (3)$$

$$X_n = G_n + W_N^{nk} H_n \quad (4)$$

This equations state that the input sequence is divided into consecutive sets of even and odd samples. In order to obtain the sets the input samples digit values are bit reversed and the resultant set is applied as input to FFT block. To calculate the inverse transform, the real and imaginary part of the input and output are swapped. From the above equations, W_N^{nk} is twiddle factor term. This twiddle factor term can be realized as butterfly operation which is the important building block of FFT algorithm [3]. The difference between Decimation In Time (DIT) and Decimation in Frequency (DIF) lies in the position of the twiddle factor multiplication, which is either performed before or after the subtraction and addition [4]. The technique use for FFT is based on divide and conquer, it will be most efficient if the input sequence is of length $N = r^p$, where N is called point, r is called radix, and p is a positive integer. An N -point FFT can be computed by using p stages of which each stage having $N/2$ butterflies [5].

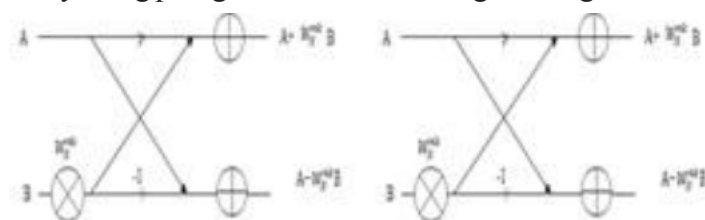


Figure 1: A radix-2 DIT and DIF Butterfly architecture

Twiddle factor generator is a key component in IFFT/FFT computation. There exist many popular generation techniques for twiddle factor; Coordinate Rotation DIgital Computer (CORDIC) algorithm, pipelined CORDIC algorithm, polynomial-based approach, ROM-based scheme, and the recursive function generators. For small lengths such as 64-point to 512 point, ROM-based is a better choice[6].Therefore in the proposed paper the implementation of pipelined CORDIC along with the synchronous parallel FFT is done and discussed in the next section.

4. CORDIC ALGORITHM

The key concept of CORDIC arithmetic is based on the simple and ancient principles of two-dimensional geometry. But the iterative formulation of a computational algorithm for its implementation was first described in 1959 by Jack E. Volder for the computation of trigonometric functions, multiplication and division [6]. CORDIC based computing received increased attention in 1971, when John Walther showed that, by varying a few simple parameters, it could be used as a single algorithm for unified implementation of a wide range of elementary transcendental functions involving logarithms, exponentials, and square roots along with those suggested by Volder [7].

CORDIC is attractive due to the simplicity of its hardware implementation, since the same iterative algorithm could be used for all the above mathematical applications using the basic shift-add operations of the form $x \pm y2^{-i}$. The conventional method of implementation of 2D vector shown in the Figure.1 using Givens rotation transform is represented by the equations [9].

$$x_{out} = x_{in} \cos \theta - y_{in} \sin \theta, \quad (5)$$

$$y_{out} = x_{in} \sin \theta + y_{in} \cos \theta. \quad (6)$$

where (x_{in}, y_{in}) and (x_{out}, y_{out}) are the initial and final coordinates of the vector respectively. The hardware realization of these equations requires four multiplications, two additions/subtractions and accessing the table stored in the memory for trigonometric coefficients. The CORDIC rotator performs 2D rotation using a series of specific incremental rotation angles selected so that each is performed by a shift and add operation iteratively.

The three basic equations of CORDIC algorithm are:

$$x_{i+1} = x_i - m \sigma_i y_i \rho^{-S_{m,i}} \quad (7)$$

$$y_{i+1} = y_i + \sigma_i x_i \rho^{-S_{m,i}} \quad (8)$$

$$z_{i+1} = z_i - \sigma_i \alpha_{m,i} \quad (9)$$

Based on the value of m the algorithm can operate in one of three configurations: Linear ($m = 0$), Circular ($m = 1$) and Hyperbolic ($m = -1$). Within each of these configurations the algorithm functions in one of two modes – rotation or vectoring. σ_i represents either clockwise or counter clockwise direction of rotation, ρ represents the radix of the number system and the shift sequence $S_{m,i}$ depends on the coordinate system and the radix of number system. $S_{m,i}$ affects the convergence of the algorithm. In rotation mode, the input vector is rotated by a specified angle, while in vectoring mode the algorithm rotates the input vector to the x-axis while recording the angle of rotation is required. The value of α_i also changes according to the configuration. Depending on the mode of operation z and y are the steering variables in rotation and vectoring mode respectively. The length of the vector increases if required micro rotations are not perfect, so in order to maintain a constant vector length, the obtained results have to be scaled by the scale factor K and it is given by the equation.

$$K = \prod_i k_i \quad (10)$$

The below flow graph represents the flow of CORDIC for computation of values:

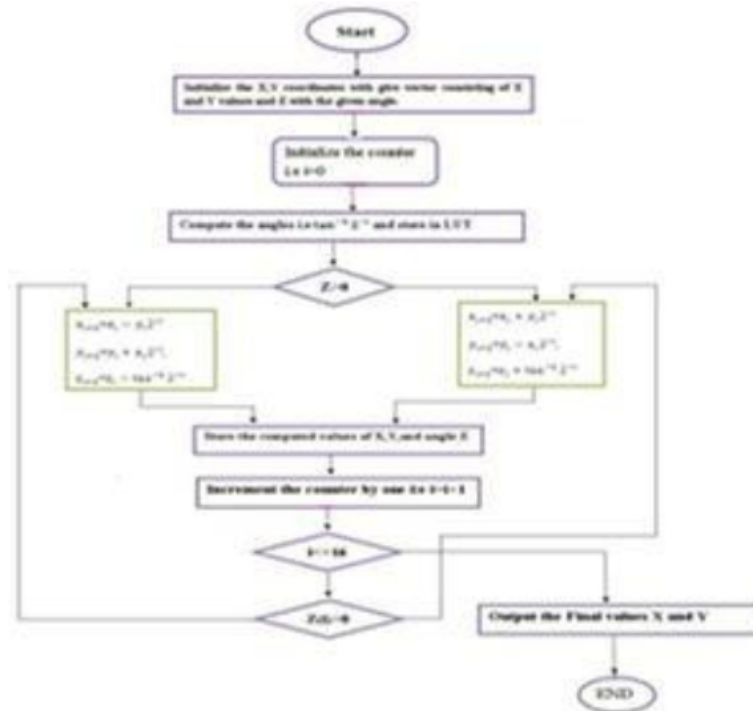


Figure 2: Flow Chart of CORDIC Algorithm

Although no popular architectures are known to us for fully parallel implementation of CORDIC, different forms of pipelined implementation of CORDIC have however been proposed for improving the computational throughput [10]. To handle latency bottlenecks, various architectures are present. Most of the well-known architectures could be grouped under bit parallel iterative CORDIC, bit serial iterative CORDIC and pipelined CORDIC architecture. Since the CORDIC iterations are identical, it is very much convenient to map them into pipelined architectures. The main emphasis in efficient pipelined implementation lies with the minimization of the critical path.

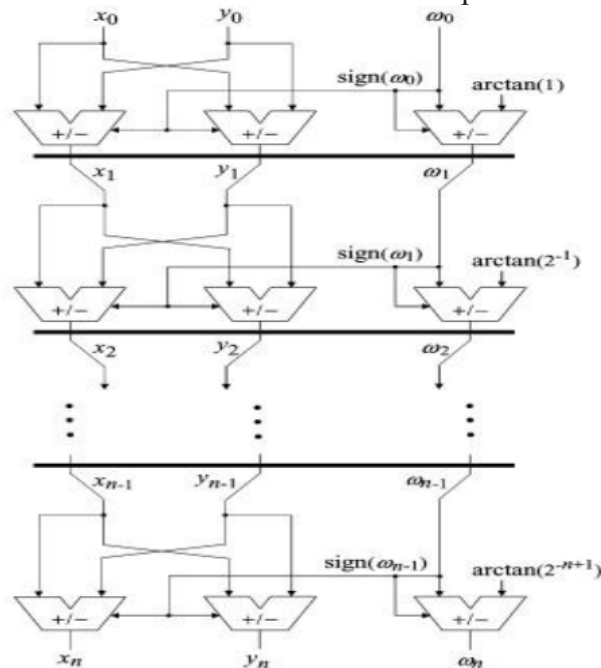


Figure 3: Basic structure of a pipelined CORDIC unit

5. IMPLEMENTATION OF 64-POINT FFT AND CORDIC

In the proposed paper as the results of 64 point FFT can't be represented exactly. So the design methodology that is used for 64-point FFT is explained by using 16-point FFT. The implementation of FFT is done using DIT-FFT algorithm. The implementation of FFT consists of bit reversing module, state machine design that acts as a controller for the total design, butter fly module and finally shifter module design.

A. Architecture of FFT: Initially in order to realize the hardware module of the FFT parallel iterative architecture is chosen as the latency for the parallel iterative architecture is less when compared to the other architectures. The values computed are stored iteratively into the intermediate registers that increase the throughput.

B. Angle Storage of FFT:

Twiddle factor is as cosine value of an angle. These angles are in decimal point form. So as the angles can't be represented directly. In Xilinx the conversion of the values need to be done for the ease of computation. The values can be represented in either fixed-point or floating point format. Representing and operating in Floating point format is tedious that consumes a lot of hardware. Therefore Fixed-point format is opted for the storage of values. The scaling of values is done by multiplying with 2 and the resultant is stored in ROM, and at the time of computation the angles are accessed based on the address.

C. Design of FFT controller:

The entire FFT module operations are controlled by using State machine as a controller. The FSM operates in 4 states that are named S_0 , S_1 , S_2 and S_3 . Each stage of the FSM performs an operation.

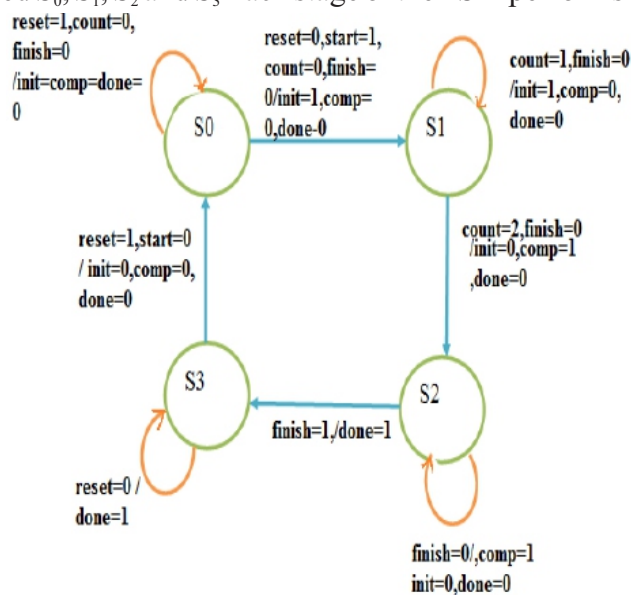


Figure 4: State machine controller of FFT Algorithm

D. Design Consideration of CORDIC in Xilinx:

In design of CORDIC element using fixed point arithmetic the accuracy and latency of the result mainly depends on the iteration count and its implementation. To achieve n - bit accuracy, the word length of x and y data path should be $(n + 2 + \log_2 n)$ bit width and for the computation of the angle θ the bit width should be $(n + \log_2 n)$. The design of CORDIC is made by considering 22 bit width of x and y along with overflow 20 bit width for angle representation.

6. VHDL SIMULATION RESULTS OF CORDIC AND FFT

The below table states the values of CORDIC obtained in Xilinx and MATLAB. On comparing both the tabulated values there is 0.01% error in one of the coordinates which is negligible. So maximum amount of accuracy is obtained through this opted methodology.

Table 1: Tabulated values of CORDIC in VHDL

Iteration Number	Value of X- coordinate	Value of Y- coordinate	Value of Angle
Iteration 1	0	262144	-61440
Iteration 2	131072	262144	47104
Iteration 3	65536	294912	-10388
Iteration 4	102400	286720	18496
Iteration 5	84480	293120	4147
Iteration 6	75320	295760	-3184
Iteration 7	79941	294584	483
Iteration 8	77640	295208	-1351
Iteration 9	78793	294905	-435
Iteration 10	79368	294752	24
Iteration 11	79081	294829	205
Iteration 12	79224	294791	-123
Iteration 13	79295	294772	-82
Iteration 14	79330	294763	-57
Iteration 15	79347	294759	-44
Final scaled value	0.184	0.682	

Table 2: MATLAB values of 16 iterations of CORDIC

Iteration Number	Value of X- coordinate	Value of Y- coordinate	Value of Angle
Iteration 1	0	1	-0.2618
Iteration 2	0.5	1	0.2018
Iteration 3	0.25	1.125	-0.0431
Iteration 4	0.3906	1.0938	0.0812
Iteration 5	0.3223	1.1182	0.0188
Iteration 6	0.2873	1.1282	-0.0124
Iteration 7	0.305	1.1237	0.0032
Iteration 8	0.2962	1.1261	-0.0046
Iteration 9	0.3006	1.125	-0.007
Iteration 10	0.3028	1.1244	0.0012
Iteration 11	0.3017	1.1247	0.0003
Iteration 12	0.3011	1.1248	-0.002
Iteration 13	0.3014	1.1248	0
Iteration 14	0.3014	1.1248	0
Iteration 15	0.3014	1.1248	-0.001

Table 3: Hardware utilization of CORDIC Algorithm

Logic Utilization	Used	Available	Utilization
Number of Slice Registers	71	93120	0%
Number of Slice LUTs	351	46560	0%
Number of Fully Used LUT- FF pairs	71	351	20%
Number of Bounded IOBS	132	240	55%
Number of BUFGCTRLS	1	32	3%

Table 4: Hardware utilization of 16-point FFT Algorithm

Logic Utilization	Used	Available	Utilization
Number of Slice Registers	942	2443200	0%
Number of Slice LUTs	2795	1221600	0%
Number of Fully Used LUT- FF pairs	729	3008	24%
Number of Bounded IOBS	962	1200	80%
Number of BUFGCTRLS	1	128	0%
Number of DSP48E1s	19	2160	0%



Figure 5: VHDL simulation result for 16 point FFT Algorithm

7. CONCLUSION

In the proposed paper the conventional implementation of CORDIC algorithm for computing the X and Y coordinates for a particular angle is done using pipelined architecture with maximum accuracy and less hardware. Along with the CORDIC 64-point FFT algorithm is also implemented with an accuracy lose of 0.4% and the final resultants are shown in the figure 5. The final excess bits of the FFT are

truncated by using truncating module that reduces the bits without the loss of accuracy. Due to the multi processing modules the output of N point FFT is obtained in $\log_2 N$ clock cycles that are shown in the above figure. The final values of FFT are stored in micro semi SRAM module.

REFERENCES

- [1] *Design, Simulation, Implementation, and Performance Analysis of a fixed-point 8 Point FFT Core for Real Time Application in Verilog HDL*, International Journal of Applied Research and Studies (IJARS) ISSN: 2278-9480 Vol 3, Issue 5 (May–2014)
- [2] Serin Sera Paul, Simy MBaby “An Efficient Design of Parallel Pipelined FFT Architecture” in IJECS Vol.3 Oct. 2014
- [3] Neha V. Mahajan, Dr. J. S. Chitode “Simple Computation of DIT FFT” IJARCSSE, Vol 4, Issue 5, May 2014
- [4] Sudha Kiran G , Brundavani P “FPGA Implementation of 256-Bit, 64-Point DIT-FFT Using Radix-4 Algorithm” Vol 3, Issue 9, September 2013
- [5] Venkata Subbarao Gutta, S. Malarvizhi “FPGA Implementation of a CORDIC-based Radix-8 FFT Processor for Real-Time Harmonic Analyzer” IJCA (0975 – 8887) in National conference on VLSI and Embedded systems 2013
- [6] J.Volder, “The CORDIC trigonometric computing technique”, IEEE Transactions on Electronic Computers, vol.EC-8, no. 8, pp 330-334, September 1959
- [7] Naveen Kumar, Amandeep Singh Sappal “CORDIC Design and Architecture”, (IJACSA) Vol. 2, No. 4, 2011.
- [8] Pipelined Parallel FFT Architectures via Folding Transformation, Manohar Ayinala, Student Member, IEEE, Michael Brown, and Keshab K. Parhi, Fellow, IEEE transactions on very large scale integration (vlsi) systems, vol. 20, no. 6, June 2012.
- [9] J M Rudagi, Srikanth, Basavaraj B Patil, Dr S Subbaraman , “Performance Analysis of Radix 4 CORDIC Processor in Rotation mode with Parallel Scale factor Computation”, IJETAE Vol 2, Issue 7, July 2012.
- [10] Amritakar Mandal* and Rajesh Mishra” Reconfigurable Design of Pipelined CORDIC Processor for Digital Sine-Cosine” Journal of Signal Processing Theory and Applications Oct.20 (2012).
- [11] Pramod, K.Sridharan “50Yearsof CORDIC: Algorithms, Architectures, and Applications”, IEEE transactions on circuits and systems I: regular papers, vol. 56, no. 9, september 2009
- [12] John F. Wakerly, Digital Design Principles and Practices, Fourth Edition, Pearson Education, Inc. 2006.
- [13] S. He and M. Torkelson, “A new approach to pipeline FFT processor,” in Proc. 10th Int. Parallel Processing Symp., 1996, pp. 766–770.
- [14] H. Wold and A. M. Despain, “Pipeline and parallel- pipeline FFT processors for VLSI implementation,” IEEE Trans. Comput., vol. C-33, no. 5, pp. 414–426, May 1984.
- [15] J.S. Walther, “A unified algorithm for elementary functions”, in: Proceedings of Spring. Joint Computer Conference, 1971, pp. 379–385.
- [16] J. W. Cooley and J. Tukey, “An algorithm for machine calculation of complex fourier series,” Math. Comput., vol. 19, pp. 297–301, Apr. 1965.
- [17] VHDL programming by J.Baskar

Supervised Learning Approach for Performance Evaluation of Digital Fundus Image Quality

P. Syed Ali Fathima Aasia¹, K. Gokulakrishnan², J. Jesu Vedha Nayahi³

¹PG Scholar, Department of Electronics & Communication Engineering, Regional Center, Anna University, Tirunelveli Region, Tirunelveli, Tamilnadu, India

²Assistant Professor, Department of Electronics & Communication Engineering, Regional Center, Anna University, Tirunelveli Region, Tirunelveli, Tamilnadu, India

³Assistant Professor, Department of Computer Science and Engineering, Regional Center, Anna University, Tirunelveli Region, Tirunelveli, Tamilnadu, India

ABSTRACT

The fundus image quality is an important parameter in medical applications. Low quality of fundus images can affect to perform a correct diagnosis. In earliest method, to estimate the fundus image quality in local image analysis technique. Drawback of this method it is only applicable for small dataset and affected some factors in retina features. To prevent those limitations we proposed a new method to determine the quality of retinal image whether it is good or bad. Initially preprocessing stage has been employed and calculates the mask. To estimate the focus measures are extracted from each image, then all focus measure values are plotted into box plot because we can predict the rules and assigned to the classifier and classify it. Finally, to obtain the classifier performance is achieved by receiver operating characteristic (ROC) curve.

Keywords: Mask, Focus Measure, Box Plot, Classification

1. INTRODUCTION

The fundus of the eye is the interior surface of the eye, opposite the lens, and includes the retina, optic disc, macula and fovea, and posterior pole. The term fundus may also be inclusive of bruch's membrane and the choroid. In one study of primates the retina is blue, green, yellow, orange, and red. only the human fundus is red. The major differences were size and regularity of the border of macular area, size and shape of the optic disc, apparent 'texturing' of retina, and pigmentation of retina [1-3]. The eye's fundus is the only part of the human body where the microcirculation can be observed directly. The diameter of the blood vessels around the optic disc is about 150µm, and an ophthalmoscope allows observation of blood vessels with diameters as 10 µm. Measuring the quality of the image is a complicated and hard process since humans opinion is affected by physical and psychological parameters [4-5]. It includes five aspects of retinal image quality .They are focus and clarity, field definition, visibility of the optic disc, visibility of the macula and artifacts. In existing methods like histogram based methods [6], image structure clustering [7] and local image analysis [8] is to verify the retina image quality in order to segmentation, used to filter bank and to extract region growing correspondence with patches. In all those methods we have several shortcomings. It is applicable for

ii) To segment the dark regions, we followed a similar approach, but first it was necessary to transform the dark regions into bright. The conversion of the original RGB (Red Green Blue) fundus image to the CMYK (Cyan Magenta Yellow Black) color space allowed us to obtain the wanted effect in the black component, as the bright objects appear as dark and the dark as bright. The black plane of CMYK color space was used in the following calculations. To obtain the binary mask of the dark regions two dynamic thresholds, t_2 and t_3 , are determined. First, the parameter t_2 corresponds to the image brightness and is obtained. Then, if t_2 is higher than a fixed value, x_1 , t_3 is determined as the intensity value corresponding to the percentage P_2 of the FOV brighter pixels extracted from the black plane image histogram. Otherwise, t_3 is determined using the percentage P_3 . This figure 3 shows that the work flow of the noise masks with black plane.

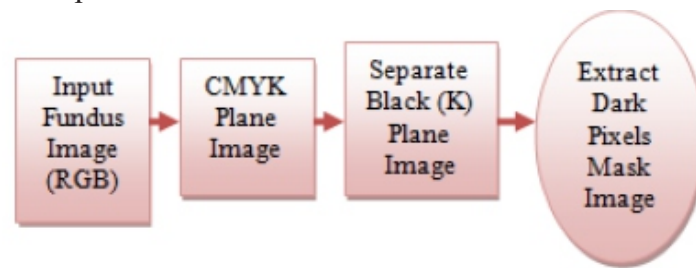


Figure 3: Work Flow of the NM with Black Plane

3. FOCUS MEASURE (FM)

It is a quantity which measures the degree of blurring of an image. Different focus measures have been proposed and used in auto focusing systems of digital cameras to determine the position of the best focused image [14-15]. In all focus measure are calculated by focused and blurred images. A good focus measure should satisfy following requirements:

1. Independence of image content.
2. Monotonicity with respect to blur.
3. Minimal computation complexity.
4. Robustness to noise.

3.1 Types of Focus Measure

- 1) Wavelet Focus Measure (WFM)
- 2) Moment Focus Measure (MFM)
- 3) Statistics Focus Measure (SFM)

3.1.1 Wavelet FM

DWT (Discrete Wavelet Transform) has minimum no. of coefficients. By restricting scale and translation. Non- redundant & bilateral transform [16].

small set of dataset, affecting retina factors like field of view, optic diameter, haze, dust and dirt, lashes, arcs, uneven illumination over macula, uneven illumination over edge, uneven illumination over optic disc, and total blink [9-12]. To overcome these limitations we introduced a new proposed method like supervised learning based on focus features is to verify the fundus image quality. The proposed method starts with calculate the mask and extracted the features like focus measure and it classifies fundus image quality through the various classifier and it is calculated the system performance.

2. MASK

Masking can describe either the techniques or materials used to control the development of a work of art by protecting a desired area from change or a phenomenon that causes a sensation to be concealed from conscious attention. There are two types of mask algorithm one is Clinically Relevant Mask (CRM) and other is Noise Mask (NM).

2.1 Clinically Relevant Mask (CRM)

The green plane image is used to calculate the FOV (field of view) mask since it corresponds to the plane with more contrast. Following, a binary mask is generated to extract the FOV. As the FOV area remains equal for all images acquired from the same equipment, a unique mask is created for each database and then used to all images [13]. We have chosen the threshold with high intensity value of that image. Figure 1 shows that the works flow of the clinically relevant mask.

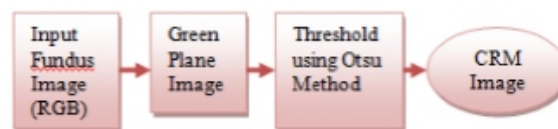


Figure 1: Work Flow of the CRM

2.2 Noise Mask (NM)

It involves two steps. The following steps are briefly described below:

- I) Green Plane Image used to obtain the binary mask of bright regions, a dynamic threshold, t_1 needs to be determined. The parameter threshold t_1 is the intensity value corresponding to the percentage P_1 of the brighter pixels extracted. This figure 2 shows that the work flow of the noise mask with green plane.

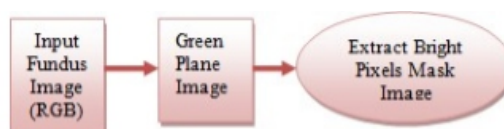


Figure 2: Work Flow of the NM with Green Plane

Forward DWT as in (1):

$$(1) \quad a_{jk} = \sum_t f(t) \psi_{jk}^*(t)$$

The discrete wavelet transform gives a multiresolution spatial frequency signal representation [17]. It measures functional intensity variations along the horizontal, vertical, and diagonal directions providing a simple hierarchical framework for interpreting the image information [18]. It is therefore natural to first analyze the image details at a coarse resolution and then gradually increase the resolution [19]. An image $f(x,y)$ at an arbitrary starting scale $j+1$ is decomposed in its low frequency subband, $W\phi(j,m,n)$ and high frequency subbands, $WH\psi(j,m,n)$, $WV\psi(j,m,n)$ and $WD\psi(j,m,n)$ where j represents the decomposition level and m and n are the columns and rows number, respectively in figure 4. Daubechies orthogonal wavelet basis D6 was used for computing FMwt. The wavelet-based focus measure used, FM (wt), is defined as the mean value of the sum of detail coefficients in the first decomposition level as in the form of the equation (2).

$$FM(wt) = (1/mn) \sum_{mn} [wH(1,m,n) + wV(1,m,n) + wD(1,m,n)] \quad (2)$$

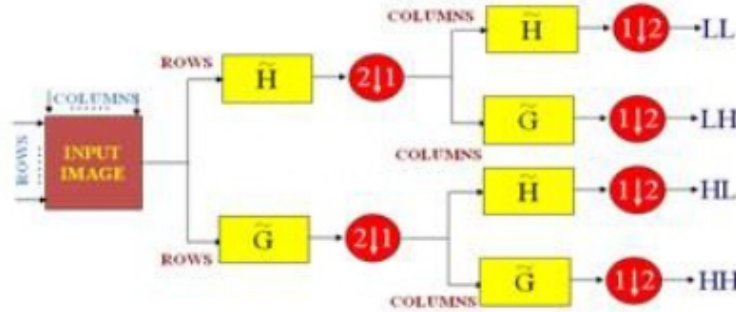


Figure 4: Wavelet Decomposition

3.1.2 Moment FM

Image moments describe image content in a compact way and capture the significant features of an image. Moments, in the mathematical point of view, are projections of a function onto a polynomial basis. They have been used successfully in a variety of applications such as image analysis, pattern recognition, image segmentation, edge detection, image registration, among others. Two View of Moment Based FM:

1. Statistical view
2. Non-Statistical view

In Statistical View ,there are several types like mean, skewness, variance, correlation, kurtosis etc .In Non Statistical View, there are several families of orthogonal moments like chebyshev, legendre, krawtchouk, dual hann, fourier-mellin, Zernike moments etc. Orthogonal moments, due to its

orthogonality property, simplify the reconstruction of the original function from the generated moments. In addition, orthogonal moments are characterized by being good signal and object descriptors, have low information redundancy and possess invariance properties, information compactness and transmission of spatial and phase information of an image. Here, we adopted a non statistical view of Zernike moment-based focus feature to —recognize blurred images [20]. Zernike moment working in optics in the 1930 derived a set of polynomials that are orthogonal over a unit disk .This figure 5 shows that the first 15 Zernike polynomials, ordered vertically by radial degree and horizontally by azimuthally degree.

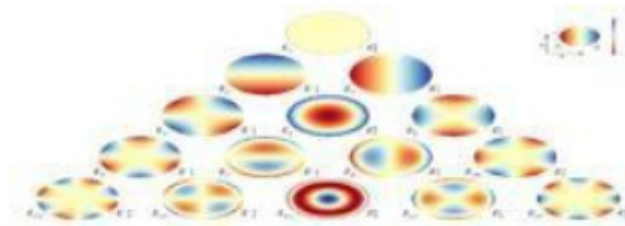


Figure 5: The First 15 Zernike Polynomials

There are specified in polar coordinates in terms of a radial component which is a polynomial of order. Their advantages: Simple rotation invariance, Higher accuracy for detailed shapes, Orthogonal, Less information redundancy. There are even and odd Zernike polynomials. The even ones and odd ones are defined as in (3) & (4).

$$Z_n^m(\rho, \varphi) = R_n^m(\rho) \cos m\varphi \quad (3)$$

$$Z_n^{-m}(\rho, \varphi) = R_n^m(\rho) \sin m\varphi \quad (4)$$

Where, m and n are nonnegative integers with $n \geq m$, φ is the azimuthally angle, here ($\varphi=0$), ρ is the radial distance. Zernike moments in terms of radial polynomial as in (5).

$$R_n^m(\rho) = \sum_{k=0}^{\frac{n-m}{2}} \frac{(-1)^k n!}{k! \frac{n+m}{2}! \frac{n-m}{2}!} \rho^{n-2k} \quad (5)$$

The zernike-based focus measure used, FM(zm), is defined as the ratio of higher order and lower order moments as in (6).

$$\text{FM(zm)} = \frac{\text{higher order}}{\text{lower order}} \quad (6)$$

3.1.3 Statistics FM

The last focus measure applied to extract image content information uses a median filter and calculates the mean energy of the difference image. The median filter is normally used in preprocessing steps of fundus images analysis algorithms to reduce noise. This filter outperforms the mean filter since it

Where, n=Number of Observations

P=percentiles (25th or 50th or 75th)

5. CLASSIFICATION

5.1 KNN Classifier

K-Nearest Neighbor (KNN) classifier is a simple supervised classification method. Suppose each sample in our data set has n attributes which we combine to form an n-dimensional vector: $x = (x_1, x_2, \dots, x_n)$. For the moment we will concern ourselves to the most popular measure of distance, Euclidean distance. The Euclidean distance between the points X and Y is calculated as in the form of equation (9).

$$\text{Dist}(X, Y) = \sqrt{\sum_i (X_i - Y_i)^2} \quad (9)$$

5.2 Fuzzy Classifier

A fuzzy classifier uses if-then rules which are easy to interpret by the user [21]. A fuzzy rule can be interpreted as a data behavior representation from which the fuzzy classifier was created, and is also known as Membership Functions (MF).

5.2.1 Fuzzy Inference Systems (FIS)

Fuzzy inference (reasoning) is the actual process of mapping from a given input to an output using fuzzy logic. The most important two types of fuzzy inference method are Mamdani and Sugeno fuzzy inference methods. Here we have chosen the Sugeno method [22] because we can predicted the limited number of rules. To generating fuzzy rules from an input- output data set, Sugeno fuzzy model was implemented into the neural fuzzy system. The most commonly used zero-order Sugeno fuzzy model applies fuzzy rules in the following

form of equation (10). This figure 8 shows that the sugeno model.

$$\text{if } x \text{ is } A \text{ and } y \text{ is } B \text{ then } z = k \quad (10)$$

Where, A and B are fuzzy sets in the antecedent,
 $z = k$ is a function in the consequent part

preserves useful details of the image. The kernel size of the median filter was chosen as in corresponding to 1/30 the height of the fundus image. By subtracting the filtered image to the original green plane image, a difference image with enhanced edges is obtained, $Idiff(x,y)$. This figure 6 shows that the work flow of the statistics based focus measure.

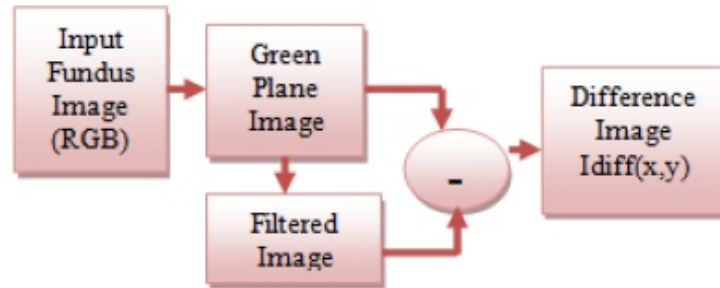


Figure 6: Work Flow of the Statistics Based Focus Measure

The statistics-based focus measure, $FM(sta)$, is calculated using the following expression as in (7).

$$FM(sta) = \sum_x \sum_y [Idiff(x,y)]^2 \quad (7)$$

Finally, all focus measure values of focused and blurred images are plotted in Box Plot.

4. BOX PLOT OR WHISKER PLOT

The box plot is defined by five data-summary values and also shows the outliers. The 25th percentile (Q1) is the value at which 25% of the data values are below this value. Thus, the middle 50% (Q2) of the data values fall between the 25th percentile and the 75th percentile (Q3). The distance between the upper (75th percentile) and lower (25th percentile) lines of the box is called the inter-quartile range (IQR). IQR is a popular measure of spread. The IQR is $Q3 - Q1$ and measures the spread in the middle 50% of the data. This figure 7 shows that the box plot or whisker plot. To construct a box plot, we need only five statistics because we can predict the rules in this range.

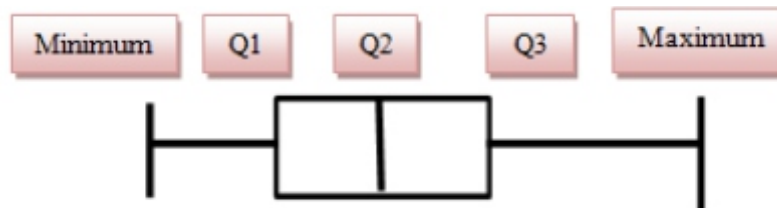


Figure 7: Box Plot or Whisker Plot

Location of percentile, L_p is calculated by using this formula as in (8).

$$L_p = (n+1)P/100 \quad (8)$$

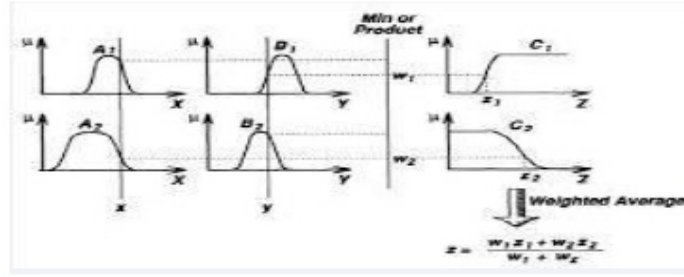


Figure 8: Sugeno Model

The system final output $f(x)$ is calculated by the weighting average of all rule outputs as in (11).

$$f_x = \sum_{i=1}^N w_i z_i / \sum_{i=1}^N w_i \quad (11)$$

5.2.2 Adaptive Neuro-Fuzzy Inference Systems (ANFIS)

A class of adaptive networks that are functionally equivalent to fuzzy inference systems. Here we adopted sugeno ANFIS. In this model every node i in this layer is an adaptive node with a node function $O_{1,i} = m_{A_i}(x)$, for $i = 1, 2$, or $O_{1,i} = m_{B_i}(y)$, for $i = 3, 4$ Where x (or y) is the input to node i and A_i (or B_i) is a linguistic label $O_{1,i}$ is the membership grade of a fuzzy set. Every node i in this layer is a fixed node labeled P , whose output is the product of all the incoming signals: $O_{2,i} = W_i = \min\{m_{A_i}(x), m_{B_i}(y)\}$, $i = 1, 2$ Each node output represents the firing strength of a rule. $O_{3,i} = \bar{w}_i = W_i / (W_1 + W_2)$, $i = 1, 2$. The single node in this layer is a fixed node labeled S , which computes the overall output as the summation of all incoming signals: $O_{4,1} = \sum_{i=1}^2 \bar{w}_i f_i$. This figure 9 shows that the sugeno ANFIS model.

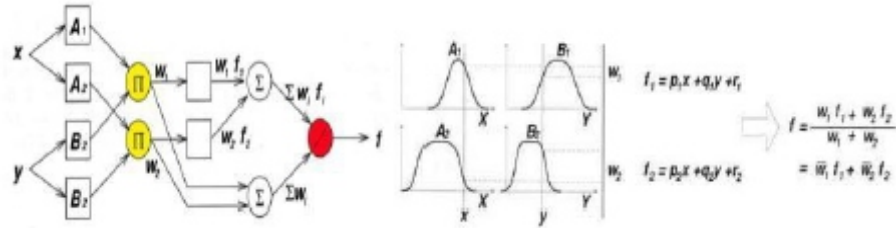


Figure 9: Sugeno ANFIS Model

6. PERFORMANCE EVALUATION

The classifier performance can be evaluated using receiver operating characteristic (ROC) analysis and the respective area under the curve (AUC). ROC curves plot the true positive fraction (or sensitivity) versus the false positive fraction (or one minus specificity). Sensitivity refers to the ability to classify an image as adequate related to focus, when it really is focused. Specificity refers to the capacity of classification of images out of focus as defocused. Accuracy was calculated by the fraction of images correctly assigned in the total number of classified images, at the operating point.

$$\text{Sensitivity} = \text{TP} / (\text{TP} + \text{FN}) \quad (12)$$

$$\text{Specificity} = \text{TN} / (\text{FP} + \text{TN}) \quad (13)$$

$$\text{Accuracy} = (\text{TP} + \text{TN}) / (\text{TP} + \text{TN} + \text{FP} + \text{FN}) * 100 \quad (14)$$

Where, TP/TN \rightarrow True Positive/True Negative

FP/FN \rightarrow False Positive/False Negative

7. RESULTS AND DISCUSSION

All processing blocks were implemented in MATLAB code, in version R2012. Database of fundus images were taken to MESSIDOR and to capture real time fundus images in Agarwal's Eye Hospital, Tirunelveli. Training set containing 382 images and the testing set containing 1072 retinal images for MESSIDOR. In real time fundus images, we have taken 100 images for training set and 175 images for testing set. The size of the MESSIDOR image is 2240×1488 and real time image is 1916×1664 .

7.1 Preprocessing Result

This figure 10 shows that the preprocessing result. The left side of the RGB image is input image for MESSIDOR and Real time images and right of the image is extract the green component.

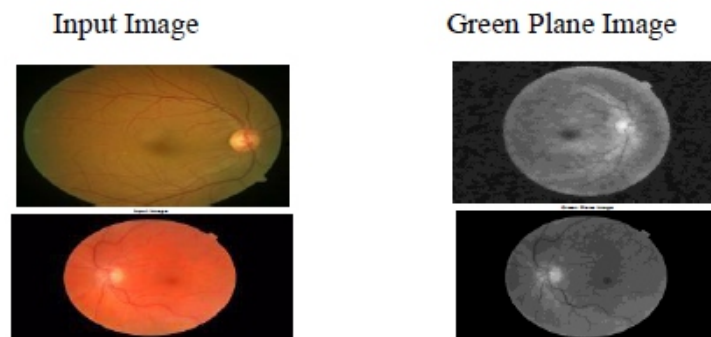


Figure 10: Preprocessing Result

7.2 Mask Result

This figure 11 shows that the mask result for clinically relevant and noise.



Figure 11: Mask Result

7.3 Focus Measure Result

The table 1 shows that the focus measure result for wavelet, zernike and statistical.

Table 1: Focus Measure Result

Database	Images	WFM	Zernike MFM	SFM
MESSIDOR	Focused	7.9E- 5	0.0546	-38
	Blurred	2.5E- 5	0.076	20
Real(Agarwal's Eye Hospital)	Focused	3.7E- 5	0.0744	17
	Blurred	1.9E- 6	0.0088	-15

7.4 Box Plot Result

This figure 12 shows that the box plot result for MESSIDOR and real images in WFM. Similarly, we have plotted the ZFM and SFM. In this plot we can predict and sorted the range of all three FM values.

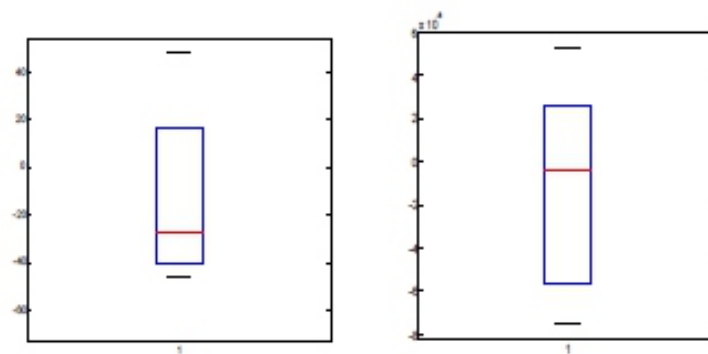


Figure 12: Box Plot Result

7.5 FIS Result

This figure 13 shows that the Sugeno FIS result.



Figure 13: Sugeno FIS Result

7.6 ANFIS Result

This figure 14 shows that the Sugeno ANFIS result.

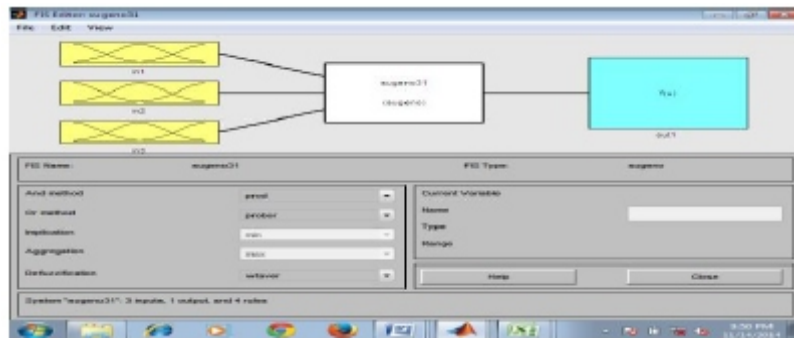


Figure 14: Sugeno ANFIS Result

7.7 ROC Plot Result

This figure 15 shows that the ROC plot result.

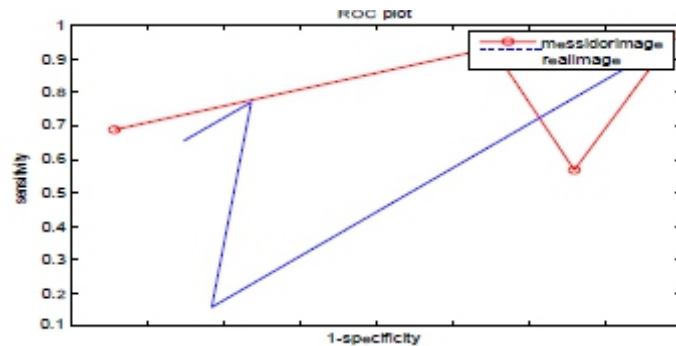


Figure 15: ROC Plot Result

7.7 Fuzzy Performance Result

This figure 16 shows that the fuzzy performance result.

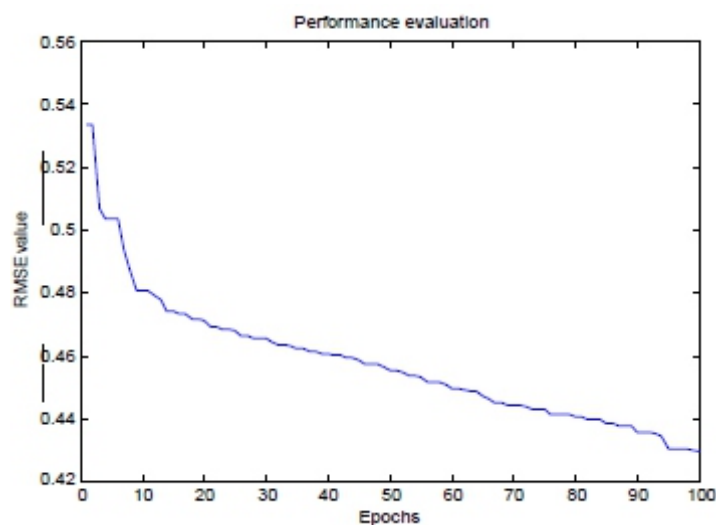


Figure 16: Fuzzy Performance Result

8. CONCLUSION

The present paper provides the preprocessing process can be done. Apply mask algorithm is to calculate the clinically relevant and noise mask, to verify the presence of uneven illumination and focus verification. Extract all focus measure value like wavelet, moment and statistics and it is marked as box plot or whisker plot. Then classifies the image quality is good or bad through classifier. Finally, KNN, Fuzzy classifiers (FIS & ANFIS) has been implemented and compared. The performance of these two classifiers has been analyzed. From that result, Fuzzy classifier gives better accuracy when compared with KNN classifier.

ACKNOWLEDGEMENT

I express my heartfelt gratitude to Dr. A. Heber M.Pharm. (Ph.D) Senior Clinical Research Manager in Dr Agarwal's Eye Hospital, Tirunelveli for providing the necessary facilities for conducting this research and his valuable suggestion its help me to greatly include this project work.

REFERENCES

- [1] P.J. Saine, —Errors in fundus photography, *J. Ophthalmic Photography*, vol. 7(2), pp. 120–122, 1984.
- [2] C.J. Heaven, J. Cansfield, K.M. Shaw, —The quality of photographs produced by the non-mydratic fundus camera in a screening programme for diabetic retinopathy, *: a 1 year prospective study Eye London England* ;7(Pt 6):787-790, 1993.
- [3] E. Trucco, —Validating retinal fundus image analysis algorithms: issues and a proposal, *Investigative Ophthalmology Visual Science*, vol. 54(5), pp. 3546–59, 2013.
- [4] M Lalonde, L. Gagnon, M.C. Boucher, —Automatic visual quality assessment in optical fundus images, *in Proceeding of Vision Interface 2001*.
- [5] T.J. Bennett & C.J. Barry, —Ophthalmic imaging today: an ophthalmic photographer's viewpoint—a review, *clinical & experimental Ophthalmology*, vol. 37(1), pp. 2–13, 2009.
- [6] S. Lee, & Y. Wang, —Automatic retinal image quality assessment and enhancement, *Proceeding SPIE*, vol. 3661, pp. 1581–1590, 1999.
- [7] D.B. Usher, M. Himaga, M.J. Dumskyj, —Automated assessment of digital fundus image quality using detected vessel area, *Proceedings of Medical Image Understanding and Analysis 2003*.
- [8] A.D. Fleming, S. Philip, K.A. Goatman, J.A. Olson, P.F. Sharp, —Automated assessment of diabetic retinal image quality based on clarity and field definition, *Investigative Ophthalmology & Visual Science* ;47:pp. 1120-1125, 2006.
- [9] T.D. Kite, —Design quality assessment of forward and inverse error diffusion halftoning algorithm, *Ph. D. thesis, University of Texas at Austin 1998*.
- [10] H. Yu, S. Barriga, C. Agurto, G. Zamora, W. Bauman, and P. Soliz, —Fast Vessel Segmentation in Retinal Images Using Multiscale Enhancement and Second- order Local Entropy, *accepted by SPIE medical imaging, Feb, San Diego, USA 2012*.
- [11] H. Bartling, P. Wanger, L. Martin, —Automated quality evaluation of digital fundus photographs, *Acta Ophthalmologica*, vol. 87(6), pp. 643–647, 2009.
- [12] J.M. Pires Dias, C.M. Oliveira, L.A. da Silva Cruz, —Retinal image quality assessment using generic image quality indicators, *Information Fusion*, vol. 19, pp. 73–90, 2014.
- [13] N. Otsu, —A Threshold Selection Method from Gray- Level Histograms, *IEEE Trans. Syst. Man and Cybern.*, pp. 62-66, 1979.
- [14] D. Veiga, —Focus evaluation approach for retinal images, *in VISAPP—VISIGRAPP, SCITEPRESS Digital Library 2014*.
- [15] X. Wang, & Y. Wang, —A new focus measure for fusion of multi-focus noisy images, *in International Conference on Computer, Mechatronics, Control and Electronic Engineering*, vol. 6, pp. 3–6, IEEE, Changchun 2010.

-
-
- [16] R.C. Gonzalez, & R.E. Woods, *Digital Image Processing 3rd ed.*, Pearson Prentice Hall 2008.
- [17] S. Jayaraman, S. .Esakkirajan, T. Veerakumar, *Digital Image Processing*, Tata McGraw Hill Education Private Limited 2013.
- [18] S. Mallat, —*A theory for multi resolution signal decomposition: the wavelet representation*,*Pattern Analysis Machine Intelligence IEEE Transaction*, vol.11(7), pp.674–693, 1989.
- [19] G. Yang, & B. Nelson, —*Wavelet-based autofocusing and unsupervised segmentation of microscopic images*,*in International Conference on Intelligent Robotics and Systems Proceedings of the IEEE/RSJ*, vol.3, pp.2143–2148 2003.
- [20] A. Khotanzad, & Y.H. Hong,—*Rotation invariant pattern recognition using Zernike moments*,*ICPR, Cambridge, UK*, pp. 326-328, 1988.
- [21] A. Hoover, & M. Goldbaum, —*Locating the Optic Nerve in a Retinal Image using the Fuzzy Convergence of the Blood Vessels*,*IEEE Trans. Med. Imag.* 22, pp.951-958 2003.
- [22] D. Nauck, & R. Kruse, —*Obtaining interpretable fuzzy classification rules from medical data*,*Artificial Intelligence Medicine*, vol.16(2), pp.149–169, 1999.
- [23] Mathworks, *Fuzzy Logic Toolbox: Adaptive Neuro fuzzy Modelling (R2012b)* 2012

Digital Wallets: A Detailed Study

Akshat Kudesia^{*}, Dr. Jyoti Pradhan^{}**

^{*} Assistant Professor, Kalinga University

^{**} Associate Professor, MATS University

ABSTRACT

The modern epoch is involving into a new momentum in payment scheme by means of digital wallets packed with cards, offers and coupons. Current atmosphere is business world, populace don't have much time to do their routine Digital works as mobile and dish TV recharge, electricity bill Digital Wallets; payment, funds and insurance payments or online Demonetization; shopping etc. In current scenario smart phones take place a vital role in the day today life of populace. This review paper reviewed a detailed study on digital wallets along with focusing on the impact of these new digital payment systems on customers and technological advancement.

Keywords: Payment System;

1. INTRODUCTION

It has been well said that every disruption creates opportunities and one this kind of disruption was the declaration of demonetization on 8th November, 2016, the honorable Prime Minister of India, Mr. Narendra Modi publicize the government preparation of demonetizing notes of 500 and 1000 with instantaneous consequence which escort to gigantic dread in all over the country. But as it said that every coin has two sides, demonetization has been functioning mostly in the support of digital wallet startups. Our nation i.e. India has perceived an exceptional boost in use of digital wallets and is gradually moving being a cashless nation. Regardless of being introduced in 2008 in India, the digital wallet been glowing acknowledged and accepted by a mainstream of the marketplace and its utilization has only amplified the recent demonetization. The digital payment structure place a significant function in this technological progression. Digital payment doorway is an e-commerce approach, which make possible the recognition as well as approval of e-payment and approved banking card payments for e-business. This doorway facilitates the relocate all the required card data between a payment gateway and the forefront processor.

There are numeral developers which are foremost to the intensification of e-payment and evolution from cash economy to e-economy. These developers comprise diffusion of web compatibility with smart phones, some of the non-banking economic organization providing digital payment systems, climb of financial technical sector and drive by government. The above mentioned aspects are constructing optimistic ambience for expansion of digital payment in India.

2. DIGITAL PAYMENTS MODES IN INDIA

- i. Banking cards
- ii. Mobile Wallets
- iii. USSD
- iv. Point of Sale (PoS)
- v. UPI
- vi. Mobile Banking
- vii. Bank pre-paid cards
- viii. Internet Banking
- ix. Bharat Interface for Money (BHIM) app
- x. Aadhaar Enabled Payment System (AEPS)
- xi. Micro ATMs

i. Banking cards:

Banking Cards are the broadly utilized payment technique along with a variety of features and advantages like safe and secure payments, ease to use, etc. The key benefit of any banking cards is that they can be utilizing to compose other kind of digital payments.

Services –

- The International banking cards may utilize across worldwide for numerous currencies
- These cards may utilize at Point of Sale machinery, ATMs, retail Shops, wallets, online transactions, and for e-commerce websites.

ii. Mobile Wallets

One can say that Mobile wallet is the digital correspondent to the physical wallet in which we hold money. Mobile wallet is online platform consent to users to maintain currency inside, as bank account. Further money is added to the „mobile wallet“ account using a banking card, online transactions from concern account or by means of cash.

Services -

- Balance Enquiry
- Transaction History
- Accept and pay money
- Profile management

iii. USSD

The modern payment service *99# implies on Unstructured supplementary service data (USSD) channel. This service permits banking transactions through fundamental attribute of mobiles, internet data facility is not required for using USSD based mobile banking. It is visualized to present economic intensification beneath banking culture in the conventional banking services.

Services -

- Balance enquiry
- Mini Statement
- Funds transfer

iv. POS (Point of sale)

PoS portal directed to those that already were set up at all retail stores where buying completed by consumers using banking cards. It is typically a portable gadget that scan and reads banking cards. On the other hand, by means of digitization the extent of PoS is growing and this portal is also accessible on mobile portal and via internet browsers. There are diverse category of PoS portal such as Physical PoS, Virtual PoS and Mobile PoS.

v. UPI

Unified Payments Interface (UPI) is a structure that amplifies numerous bank accounts into a sole mobile app of concern bank, integration various banking features, flawless fund routing & commercial payments into one lid. It also furnish to the “P2P” gather application which can be programmed and remunerated accordance with necessity and ease. All banks offer individual UPI App based on handset platform.

Services—

- Balance Enquiry
- Transaction History
- Send / Pay Money
- Add bank account
- Change / Set MPIN
- Notifications
- A/c Management

vi. Mobile Banking

Mobile banking is a broad phrase utilized for the wide range of services. Mobile banking is about to the practice of functioning financial or banking transactions via smart phone. The range of mobile banking is growing with the launch of numerous mobile wallets, web based payment application, UPI. Lots of financial institutes have their individual apps and consumers can utilize the similar to accomplish banking transactions at one click.

vii. Bank pre-paid cards

Bank prepaid card is a payment gadget on to which one can stack money for purchasing. Such kind of card might not be associated with bank account of the consumer. On the other hand, a debit card issued by the bank is allied with the consumer's bank account.

Services -

- Balance Enquiry
- Transaction history
- Add money
- Bank A/c
- All Cards
- Accept Money
- Pay money
- Another wallet (mobile no.) with same provider
- Pay merchant
- Bar Code reader
- Cash-Out (Cash withdrawal)
- Touch and Pay

viii. Internet Banking

Internet banking depicts the method of executing banking transactions online. These may consist of various services like opening new FD/RD, transferring amounts, Bill payments, etc. Internet banking is also illustrated as virtual banking or e-banking. Some of the financial transactions are Electronic Clearing System (ECS) National Electronic Fund Transfer (NEFT), Real Time Gross Settlement (RTGS), and Immediate Payment Service (IMPS).

ix. Bharat Interface for Money (BHIM) app

The BHIM app (Bharat Interface for Money) permits users to pay using the UPI application. It can also be utilized in alliance with UPI and banking transactions can be carried out using a virtual payment address (VPA). Anyone can connect their bank account with the BHIM interface in a very easy way. One more facility is to connect multiple accounts. This app can be utilized by any person having a mobile number, debit card and an authentic bank account. Funds can be transferred to various bank accounts, virtual addresses or to an Aadhaar number.

x. Aadhaar Enabled Payment System (AEPS)

Abbreviation as Aadhaar Enabled Payment System can be used for banking transactions like available balance enquiry, fund withdrawal, fund deposit, payment transactions, Aadhaar to Aadhaar fund transfers, etc. All the above mentioned transaction and other services are accomplished through a banking correspondent based on Aadhaar authentication.

xi. Micro ATMs

Micro ATM is a mechanism that is utilized by a large volume of Business Correspondents (BC) to convey essential banking services. This platform will facilitate Business Correspondents like a local grocery shop vendor to perform instantaneous transactions. The basic transaction types supported by micro ATM are:

Fund transfer, Deposit, Withdrawal, and Balance enquiry

3. LITERATURE REVIEW

Some of the studies on digital wallets are as follows –

Roopali batra et al.'s [2] research, intend to experientially observe the acceptance of digital wallets by of the respondents. A study of client opinion, prototype preferences used by consumers and contentment level about digital wallets is accomplished based on an analysis of 52 respondents. In addition with this analysis it also recognizes the hurdles and challenge to the acceptance of digital wallets. To attain the aforementioned function a logical opinion poll was directed to respondents in which they were asked over a variety of questions regarding acceptance of digital wallets. The outcomes specify that there present an enormous intact marketplace for digital wallets. Less time consumption and simplicity of usage were turn out to be the core cause for using wallets. Safety matters like cash loss and less usability for global transactions are the major hurdles to its acceptance.

Pawan Kalyani [3] illustrates research paper concentrate on the paperless e-currency transaction that is getting trendy globally, India is a emergent market and numerous services are accessible on web and they receive payments online, but it also analyze number of people are truly relaying on it, Number of people are utilizing it for online transactions furthermore, the research is based on the survey answer by respondents. Research reviewed that populace are utilizing only some services typically for recharging mobile bill, DTH bills, but there are lots of services which are already utilized in the global market. The knowledge and realistic usability of the E-wallet is short, that must be amplified by adding extra value added services to it.

Taheam, K. et al. [4] demonstrate outcome from the research which tinted on different aspects that inspired people to use digital wallets for online transactions. It is found that people in Punjab utilizing digital wallets because of the objects of security & controllability, communal sway & worth and necessitate for performance improvement. This review specifies that people of Punjab use any kind of digital wallet because of these recognized motives.

Madhu Chauhan et al.[5] researched regarding e-payments particularly mobile wallets. After demonetization, there is an incredible increase in number of e-payments. This paper particularly marks undergraduate learners and depicts their favored approach of payment. It also put forwards a few steps that must be consider for improvement of e-payment conveniences.

A research illustrates as per Ministry of Finance statement (December 2016) on Digital payment, economic incorporation is one of the leading challenges in front of India. 53 percent of Indian populace had admittance to official financial services. In this perspective, digital payment can be active as accelerator to economic incorporation. Growing accessibility of mobiles, accessibility of network communications, even out of 3G and 4G networks and huge trade eco structure are the significant enablers of digital payment in India. It is advance hold up by the synchronized efforts of industry, regulator and government. As per RBI's report „Vision 2018“ four pronged strategy focusing on regulation, robust infrastructure, effective supervisory mechanism and customer centricity has been adopted to push adoption of digital payment in India. [6]

4. DRIVERS AND BARRIERS OF DIGITAL WALLETS ADOPTION

In India acceptance of digital payments are promoted by the Government. But citizens of India are accepting gradually these digital payments. Table 1 includes causes of drivers and barriers of digital payment system.

Table 1. Drivers and barriers of Digital Payment system[1]

Drivers	Barriers
Contribution value added for clients, traders, network operators, financial organizations and other contributors in the ecosystem.	Complex value-chain with lack of cooperation.
Easy-to-use	Financial Regulation.
Buying is more convenient	Inaccessibility of an extensive series of mobile payment competent handset.
Offers variety of options	Limited retailers
Less time required	Out of Battery then no purchasing
Business opportunities and greater potential revenue.	System Outages, supporting technologies

5. DIGITAL WALLETS AVAILABLE IN INDIA

Digital payment system starts in India few years ago. In starting it was stated that citizen of India is not ready for digital payment system. In early days digital payment was status symbol. But during and after demonetization citizens of India are partial forced for using digital payment due to cash shortage. Banks and payment agency saw the opportunity of business in this domain. Now a day, most of the banks came up with their wallet and private players also came with payment bank concept. Table 2 summarizes various wallets offered for digital payment.

Table 2. Wallets offered by various agencies.

Airtel Money:	Ezetap:
• Recharge prepaid and postpaid accounts	• Bangalore based digital payment solution
• Online shopping	• Accept card payments via electronic devices
• Safe because of secret 4-digit mPin	• Customers get e-receipts through an SMS or email
HDFC PayZapp	Citrus Pay:
• easily compare flight and hotel tickets	• offers a Citrus wallet for customers as well as payment solutions to businesses
• buy music or pay bills with the app	• strong base of 800+ million customers
• Simple connect your debit/credit card	
ICICI Pockets	JioMoney
• VISA powered	• Consumer receives great discounts and offers
• used on any Indian website	• bookmark frequently visited retailers so shopping can be made quicker
• transfer money to email ids, WhatsApp contacts	
Freecharge	Citi MasterPass
• target the youth in all their promotions	• free digital wallet
• equivalent amount of coupons given for every recharge you make	• processing is fast
	• securely store all details related to the payment card

JusPay:	Mobikwik:
• payment browser with over 650+ transactions in a day	• Gurgaon based e-wallet payment system
• make payments quickly via cards with 2 clicks	• enables users to recharge, pay bills, and make third-party purchases with one tap
LIME:	MomoeXpress:
• Launched by AXIS	• Bangalore based digital wallet in India
• First mobile app to integrate wallets, shopping, payments, and banking	• paying for your rickshaw ride to salons & spas, there are over 3000 outlets available at your disposal
MoneyonMobile:	Oxigen:
• multilingual app	• FinTech Company
• authorized by the Reserve Bank of India	• Along with making online purchases and paying bills, you can also send gift cards to your dear ones
• buy goods, products, and services from registered merchants	
Paytm:	State Bank Buddy:
• currently the largest mobile wallet app in India	• online wallet in India that's available in 13 languages
• accepted almost everywhere	• Users who don't have SBI accounts can send money via Facebook, or to other bank accounts, book hotels or movie tickets and much more
PayUmoney:	PayMate
• free payment gateway solution for merchants to collect payments from customers via debit/credit cards or net banking, and more	• launched PayPOS
• offer SMS and email invoicing for merchants that do not have a website	• app for small business owners to receive payments conveniently via debit cards and credit cards

6. CONCLUSION

Digital wallets somewhere are and will be the futures of currency. Currently the days have come when „Kirana“ store, chemist shop and restaurant in India accepted the cashless transaction through digital wallets. Technical expertise will transform the whole thing and it shows the way for future outlooks particularly in financial ground. Being a new product which is almost a concerned with technical background, consumer education is essential so it is the responsibility of all the digital wallet financial institutes to tutor them. With the help of this, more rapidly digital wallet will be an immense triumph in global market.

REFERENCES

- [1] http://cashlessindia.gov.in/digital_payment_methods.html
- [2] Roopali Batra, Neha Kalra, "Are digital wallets the new currency?", *Apeejay Journal of Management and Technology*, Vol.11, Issue 1, January 2016.
- [3] Pawan Kalyani, "An Empirical Study about the Awareness of Paperless E-Currency Transaction like E-Wallet Using ICT in the Youth of India", *Journal of Management Engineering and Information Technology (JMEIT)* Vol. 3, Issue 3, Jun. 2016, PP18-41.
- [4] Taheem, K., Sharma, R., & Goswami, S. (2016). Drivers of Digital Wallet Usage: Implications for Leveraging Digital Marketing. *International Journal of Economic Research*, Vol. 13, Issue 1, PP 175-186.
- [5] Madhu Chauhan, Isha Shingari, "Future of e-Wallets: A Perspective From Under Graduates", *International Journals of Advanced Research in Computer Science and Software Engineering*, Vol. 7, Issue 8, 2016, PP 146-150
- [6] KPMG (2017) *Digital Payment-Analyzing the cyberspace*.

Performance Evolution and Selection of Controllable Process variables in ECM for Al, B4C Metal Matrix Composites

Bedasruti Mitra^{*} Sandeep Kumar^{}**

^{*} Assistant System Engineer, TCS, Hyderabad, India

^{**} Faculty of Mechanical Engineering, M. Kumarasamy College of Engineering,
Karur, Tamilnadu, India

ABSTRACT

In recent years, the need for light weight MMCs products are becoming more valuable in aerospace, electronics, nuclear power plants and defence industries because of their specific properties. The machining of MMCs is a big Electrochemical concern and still an area of research. Al, B4C is one of the Machining; widely accepted MMC having specific properties like MMCs; wear and impact resistance. This composite shows MRR; difficulty while machining with non- conventional SR; processes due to various reasons such as higher surface roughness, tool wear rate and machining cost. In this Multi-parametric experimental work, ECM has been selected for machining optimization. of Al,B4C composite to get better product quality & satisfactory machining characteristics. The voltage, feed rate, B4C % age of reinforcement and electrolyte concentration were selected as process constraints to conduct experimental trials. The Surface roughness, MRR and radial over cut were considered as output responses. The experimental outcomes were optimized by multi- parametric optimization using DoE and Grey relational analysis. The optimized parameters by multi-parametric optimization showed the considerable improvement

1. INTRODUCTION

ECM (Electro Chemical Machining) generally known as anodic cutting is the latest and most useful modern machining. Because of its machining capability of machining metal alloys, fragile parts, complex shapes and insignificant tool wear; ECM is mostly utilized to machine harder and tougher materials with stress free conditions. ECM process is the reverse process of Electroplating (i.e. If two electrode plates are placed in a bath containing conducting liquid and direct current is supplied across them, the metal depletes from the anode (+ve) plate to the cathode (-ve) plate) with certain modification. [1,2]

The ECM process used a shaped tool or electrode which is linked to the cathode (-ve) terminal & workpiece is connected to the anode (+ve) terminal. The spark gap of 0.05 to 0.03 mm is kept between the tool electrode and material which allows the passage of an electrolytic neutral salt solution (i.e. Sodium chloride, sodium nitrate and sodium chlorate) between the gap. D.C. of ranges from 1-20 V current is supplied to the tool and work piece. An electronic ion is pulled from the material surface when sufficient energy, i.e. 6eV is available. The -ve ions present in the electrolyte solution reacts with the +ve ions and form metallic hydroxide compounds. Therefore, the metal is anodically dissolved with the formation of sludge and MRR is generated by “Faraday’s Law of electrolysis” as shown in Fig 1. [2, 5]

MMCs are the composites which are reinforced with fibers & ceramics and consists metal matrices, reinforced with fibers. It consists of the primary phase, i.e. metal matrix & secondary phase i.e. reinforcement. The primary phase consists of the bulk form of composite material; it holds the imbedded phase and conceals it. When an external force is employed primary phase distribute the force with secondary phase. The secondary phase increases the properties of the material, i.e. increase in strength, improvement in corrosion and shock resistance. In this experimental study, Al (matrix metal) is primary phase and B₄C reinforced metal is the secondary phase. [5, 8]

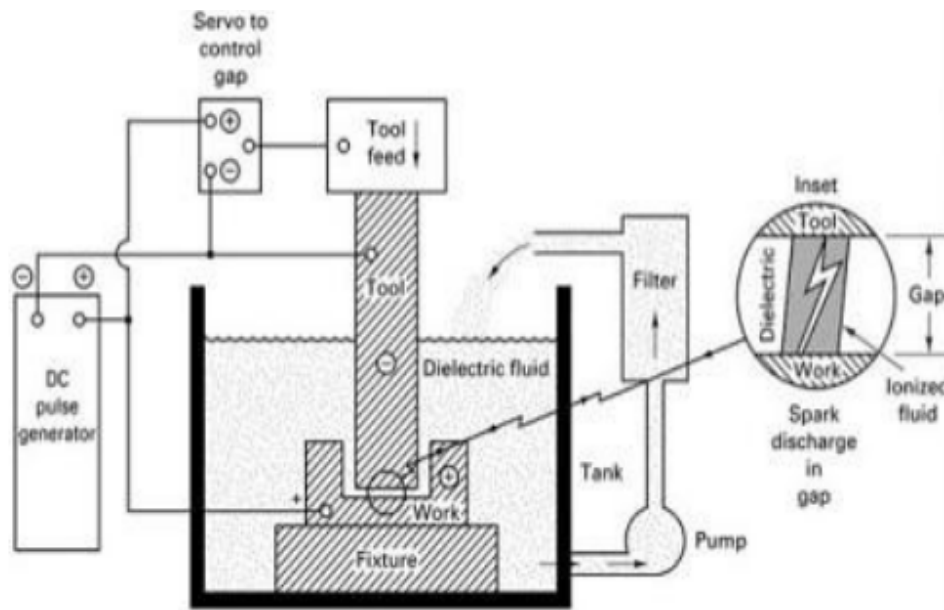


Fig.1. Schematic view of ECM

The Aluminium metal matrix has several industrial applications and it deals with two types of reinforcements i.e. AL₂O₃ (aluminium oxide) and SiC (silicon carbide). Because B₄C has a low specific gravity, hardness below than the diamond and boron nitride & thermal expansion similar to the SiC, therefore, B₄C is used as an alternative to SiC and AL₂O₃. It has advantages for various applications such as wear and impact resistance and neutron absorption; therefore, B₄C is used in reinforcement phase. The interfacial reactions in Al composites depend mainly on fabrication method, chemical composition of the matrix and condition of fabrication. The properties of the interface changes by composition methods utilized. [9-13]

Raj Kumar et al investigated the effect of D.C. voltage by using NaCl, NaNO₃ aqueous solution at high speed. The authors concluded that 10-25 V voltage is suitable for ECM. [5] Neto et al investigated the effect of feed rate on valve steel and concluded that the value for SR decreases with the lower feed rate. [6] Ashokan et al investigated the ECM parameters using grey relational combined with an ANN method to analyze the effect of machining parameters such as current, voltage, flow rate and gap of

hardened steel. [4] Rao et al concluded that the rate of MRR increase with feed rate, voltage and electrolytic concentration & decrease with %age of reinforcement. [11] Senthil Kumar et al demonstrated a mathematical model by using RSM and NSGA for improvement of ECM parameters for Al, SiC composites. [10]

Based on the literatures, it is found that no plausible works are conducted on multi-parametric optimization using DoE and Grey relational method of machining Al2B4C metal matrix composite in the ECM process [9, 10]. Taguchi method, TOPSIS and GA (Genetic Algorithm) had been utilized to optimize the process parameters in ECM process. [17-20]. Design of experiments (DoE) and regression analysis was performed by the application of Taguchi’s orthogonal array. In this work, MRR, Surface roughness and radial over cut has been considered. Even though, the goal of the ECM could be to acquire the supreme MRR after machining suitable parameters. The said problem has been described by multi-objective optimization by using Grey relational analysis.

2. EXPERIMENTAL PLAN

Design-of-experiments (DoE) needs cautious scheduling, practical layout of the trials, Taguchi has identical procedures for every DoE application steps and also DoE can dramatically decrease the amount of trials. Thus,

Table 1. Allocated values of ECM parameters and their levels

	Parameter	Units	Level-1	Level-2	Level-3
A	Voltage (V)	Volts	12	16	20
B	Feed rate (F)	mm/min.	0.2	0.6	1
C	Electrolyte concentration	g/lit.	10	20	30
D	%age of Reinforcing	Wt%	2.5	5	7.5

The four important machining parameters, i.e. Voltage (V), Feed rate (F), electrolyte immersion and %age of reinforcing had selected for the governing parameter, and each parametric quantity had three levels denoted by level 1, level 2 and level 3, as designated in the Table 1. These important parameters were selected from the previous literatures.

2.1. Running Experiment

MCMAC Meta Tech Electrochemical machine was used for the experimentation as shown in Fig. 2. EN1706 aluminium alloys circular bar having a 25mm diameter was used as a primary metal. The aluminium alloy was reinforced by B4C secondary phase in different Wt% through liquid state processing (i.e. Squeeze casting). In this process, the molten metal is forced into a fibrous and squeezed

until solidification is accomplished. As per DoE the experiments were conducted with a 20 V rated ECM machine and the work piece was used in the form of a cylinder. The workpiece and the electrodes were linked up with +ve and -ve polarity in the D.C power source respectively. Circular cross sectional Copper tool with internal hole for the electrolyte flow was used for experimental work. The values for surface roughness were measured with the help of the surface roughness tester. The mass of the workpiece before and after machining for every trial run was measured with digital weight-balance (up to 0.001 gram accuracy).



Fig.2. Meta Tech Electrochemical Machining Setup

The mathematical relation used to evaluate the Surface roughness (SR) is given below:

$$SurfaceRoughness(Ra) = \frac{1}{L} \int_0^L |Z(x)| dx \quad (\mu m) \quad (1)$$

Where; Ra is the surface roughness value measured in μm , L = evaluation length; Z (x) = profiles height function.

The formula used to find the Radial over cut (ROC) is given below:

$$ROC = \frac{DIA. \text{ of hole in material} - DIA. \text{ of tool}}{2} \quad (mm) \quad (2)$$

The formula used to find the Workpiece Removal Rate (MRR) is given below:

$$MRR = \frac{Weight \text{ of material removal}}{Time} \quad (g / min) \quad (3)$$

After machining of AlB4C composite, radial over-cut of the material was evaluated with a digital vernier caliper. Each sample was evaluated by thrice and mean values were considered.

3. Taguchi Analysis

To design the experiments, the first step is selection of appropriate Orthogonal Array, Assign each factor to columns, identify each trial circumstance, and decides the set up and repeating of trial circumstances. An OA Design matrix table is generated.

3.1. Experimentation

In the present experimentation work, $L_{27} (3^3)$ OA was chosen. L_{27} Orthogonal Array has 27 parametric combination therefore the total number of 27 experiments were conducted to measure the interactions between the various factors. The parameter combinations using the L_{27} or OA are shown in Table 2.

Table 2. DoE (Design of Experiment) Matrix of $L_{27} (3^3)$ Orthogonal array (OA) and measured values for output responses

Sl. No.	Voltage (A)	Feed Rate (B)	Electrolyte Concentration (C)	%age of Reinforcing (D)	Surface Roughness (μm)	ROC (mm)	MRR (g/min.)
1	12	0.2	10	2.5	4.95	0.97	0.269
2	12	0.2	20	5	5	0.95	0.337
3	12	0.2	30	7.5	4.6	0.8	0.227
4	12	0.6	10	2.5	4.92	0.76	0.353
5	12	0.6	20	5	4.5	0.65	0.448
6	12	0.6	30	7.5	4.73	0.8	0.42
7	12	1	10	2.5	4.6	0.68	0.689
8	12	1	20	5	4.36	0.65	0.545
9	12	1	30	7.5	4.23	0.64	0.703
10	16	0.2	10	5	4.9	0.92	0.321
11	16	0.2	20	7.5	4.8	0.95	0.329
12	16	0.2	30	2.5	4.3	1.04	0.488
13	16	0.6	10	5	4.55	0.77	0.379
14	16	0.6	20	7.5	4.4	0.7	0.302
15	16	0.6	30	2.5	4	1	0.583
16	16	1	10	5	4.3	0.76	0.615
17	16	1	20	7.5	4.35	0.71	0.619
18	16	1	30	2.5	3.6	0.94	0.812
19	20	0.2	10	7.5	5.5	0.92	0.282
20	20	0.2	20	2.5	4.8	1.1	0.599
21	20	0.2	30	5	4.6	1.17	0.6
22	20	0.6	10	7.5	5.21	0.86	0.526
23	20	0.6	20	2.5	4.9	1.03	0.688
24	20	0.6	30	5	4.5	1.08	0.73
25	20	1	10	7.5	5	0.65	0.68
26	20	1	20	2.5	4.4	0.99	0.887
27	20	1	30	5	4	1.1	0.944

For accurate measurements minimum three values were taken for each specimen and the mean value was selected. The mean values of the SR, Radial over cut and MRR are shown in the table 3.

4. TAGUCHI ANALYSIS

OE is the first step of experimental work and a statistical technique introduced by R.A. Fisher (1920). In DOE the change in corresponding output variables is measured by changing the values of Input

variables and used to find the most efficient and effective conclusions by designing, planning and organizing.

To design the experiments, the first step is selection of appropriate Orthogonal Array, Assign each factor to columns, identify each trial circumstance, and decides the order and repetitions of trial circumstances. Taguchi analysis is used for the selection of best-optimized parameter value for the individual process parameter and to measure the influence of each parameter at different levels. [10]

The ANOVA mathematical relation (Lower is the better) used to evaluate the S/N ratio of surface roughness and radial over cut is given below:

$$\eta_{LB} = -10 \log \left[\frac{1}{n} \sum_{i=1}^n \frac{1}{y_i^2} \right] \quad (4)$$

The ANOVA mathematical relation (Higher is the better) utilized to evaluate the S/N ratio of the Material removal rate (MRR) is given below:

$$\eta_{HB} = -10 \log \left[\frac{1}{n} \sum_{i=1}^n y_i^2 \right] \quad (5)$$

The S/N ratio η_{ij} for the i^{th} performance characteristics in the j^{th} experiment is evaluated by the following relation:

$$\eta_y = -10 \log[L_y] \quad (6)$$

Where; y = observed data and n = no. of trials

4.1. Dominance of Input parameters on Surface roughness

The main effect plot for means (for surface roughness) generated by Minitab 16 Software is shown in the Figure 3. This graph indicates the effect of individual input parameters on the surface roughness. In this analysis "Smaller is better" S/N ratio was used. This graph shows the best optimized values for surface roughness.

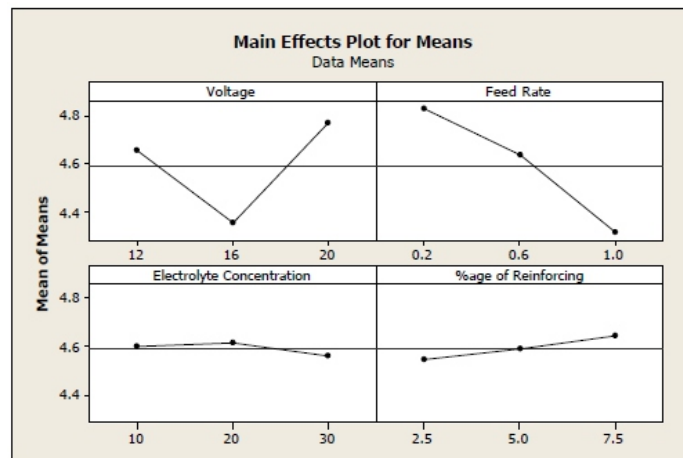


Fig.3. Main effect plot for means (Surface Roughness)

The best optimized level values for surface roughness are:

Optimized Parameters	Voltage (A)	Feed Rate (B)	Electrolyte Concentration (C)	%age of Reinforcing (D)
Level	2	3	3	1

Table 3. Surface Roughness Response table for means (Smaller is better)

Level	Voltage (A)	Feed Rate (B)	Electrolyte Concentration(C).	%age of Reinforcing (D)
1	4.654	4.828	4.601	4.544
2	4.356	4.634	4.617	4.589
3	4.768	4.316	4.56	4.644
Delta	0.412	0.512	0.057	0.1
Rank	2	1	4	3

The surface roughness response table for means is shown in the Table 3. This table represents the most significant parameter and least significant parameter for surface roughness (SR). The table clearly indicates that the feed rate and voltage are the most significant parameters for surface roughness whereas the %age of reinforcing and electrolyte concentration has the least significance.

The influence on surface roughness in relation to change of ECM process parameters is illustrated in Figure 4.

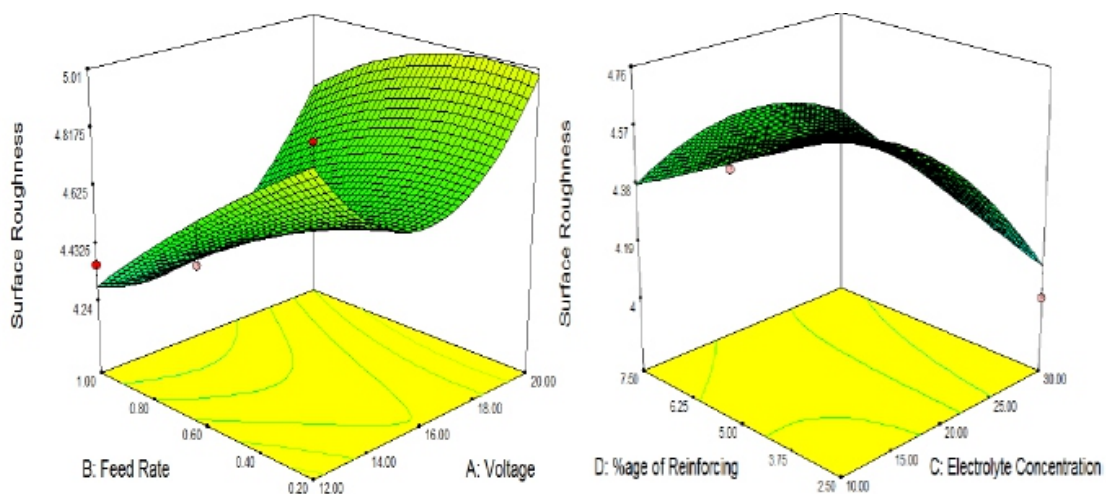


Fig.4. Influence on surface roughness in relation to change of (i) Voltage and feed rate and (ii) electrolyte concentration and %age of reinforcing

4.2. Dominance of Input parameters on ROC

The main effect plot for means (for ROC) generated is shown in the Figure 5. This graph indicates the effect of individual input parameters on the ROC (Radial over Cut). In this analysis "Smaller is better" S/N ratio was used. This graph shows the best optimized values for ROC.

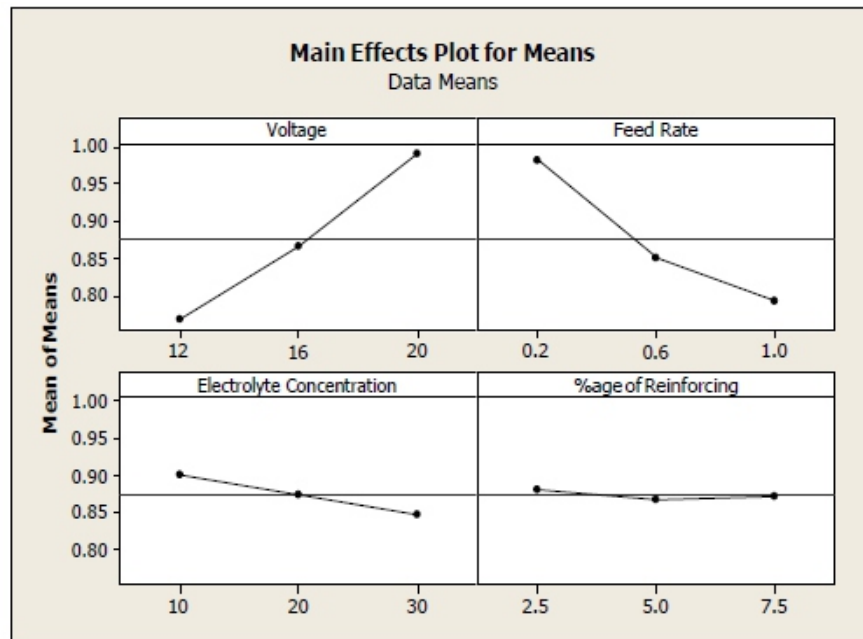


Fig.5. Main effect plot for means (ROC)

The best optimized level values for ROC are:

Optimized Parameters	Voltage (A)	Feed Rate (B)	Electrolyte Concentration (C).	%age of Reinforcing (D)
Level	1	3	3	2

Table 4. ROC Response table for means (Smaller is better)

Level	Voltage (A)	Feed Rate (B)	Electrolyte Concentration (C).	%age of Reinforcing (D)
1	0.7667	0.98	0.9	0.8811
2	0.8656	0.85	0.8733	0.8678
3	0.9889	0.7911	0.8478	0.8722
Delta	0.2222	0.1889	0.0522	0.0133
Rank	1	2	3	4

The ROC response table for means is shown in the Table 4. This table represents the most significant parameter and least significant parameter for ROC. The table clearly indicates that the voltage and feed rate has the most significance on ROC whereas the %age of reinforcing has least significance.

The influence on ROC in relation change of voltage, feed rate, electrolyte concentration and %age of reinforcing levels is illustrated in Figure 6.

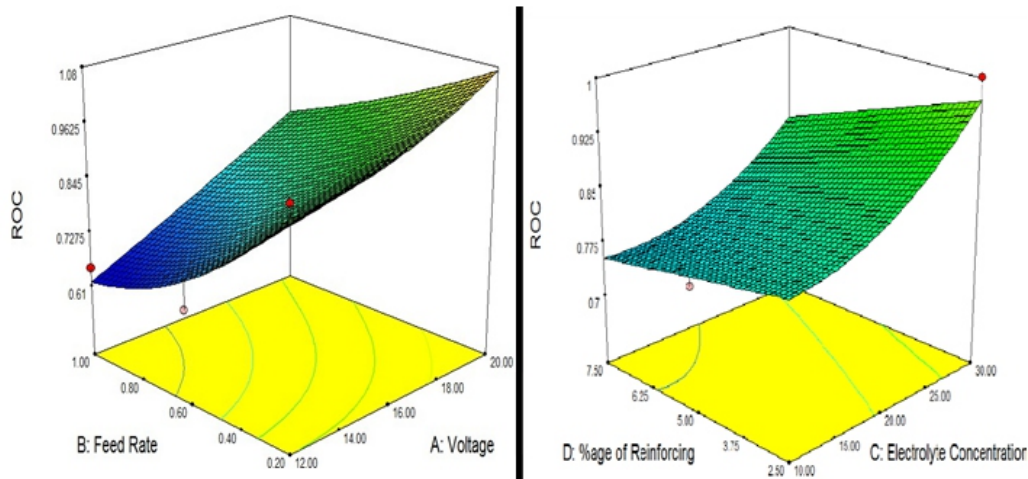


Fig.6. Influence on ROC in relation to change of (i) Voltage and feed rate and (ii) electrolyte concentration and %age of reinforcing

4.3. Dominance of Input parameters on MRR

The main effect plot for means (for MRR) generated is shown in the Figure 7. This graph indicates the effect of individual input parameters on the MRR (Material removal rate). In this analysis "Larger is better" S/N ratio was used. This graph shows the best optimized values for MRR.

The MRR (Material removal rate) table for means is shown in the Table 5. This table represents the most significant parameter and least significant parameter for MRR. The table clearly indicates that the feed rate and voltage has the most significance on MRR whereas the electrolyte concentration has the least significance.

The best optimized level values for MRR are:

Optimized Parameters	Voltage (A)	Feed Rate (B)	Electrolyte Concentration (C).	%age of Reinforcing (D)
Level	3	3	2	3

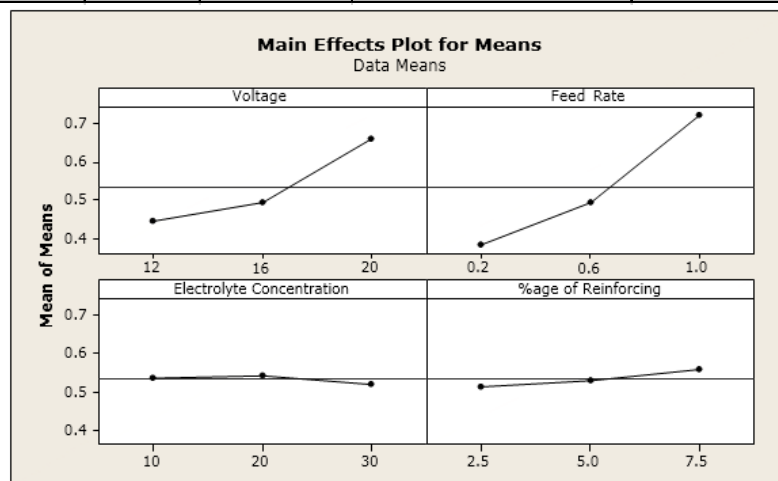


Fig.7. Main effect plot for means (MRR)

Table 5. MRR Response table for means (Larger is better)

Level	Voltage (A)	Feed Rate (B)	Electrolyte Concentration (C)	%age of Reinforcing (D)
1	0.4434	0.3836	0.5359	0.512
2	0.4942	0.4921	0.5411	0.5276
3	0.6596	0.7216	0.5202	0.5577
Delta	0.2161	0.338	0.0209	0.0457
Rank	2	1	4	3

The influence on MRR in relation to change of ECM process parameters is illustrated in Figure 8.

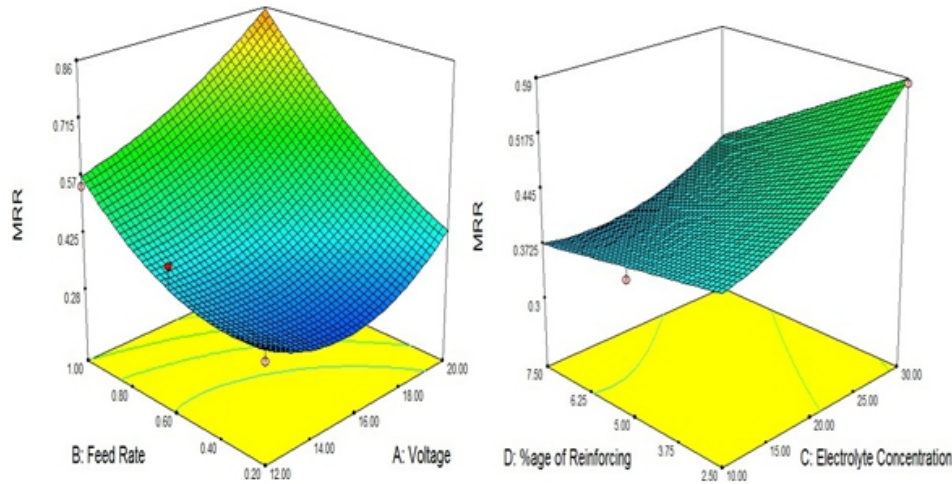


Fig.8. Influence on MRR in relation to change of (i) Voltage and feed rate and (ii) electrolyte concentration and %age of reinforcing

5. MULTI-PARAMETRIC OPTIMIZATION USING THE GREY RELATIONAL METHOD

The steps used for multi-parametric optimization using the Grey relational analysis is discussed below; [18]

a) Normalization of the all experimental results: The normalized values for output responses were calculated by using the standard formula:

$$\text{Normalized Results } (X_{ij}) = \frac{(y_{ij}) - (\min_j y_{ij})}{(\max_j y_{ij}) - (\min_j y_{ij})} \quad (7)$$

Where,

y_{ij} = i^{th} experiment results in j^{th} experiment.

Table 6. Calculated values for Grey Relational Grade

Sl. No.	Voltage (A)	Feed Rate (B)	Electrolyte Concentration (C)	%age of Reinforcing (D)	Grey relational Grade
1	12	0.2	10	2.5	0.402732959
2	12	0.2	20	5	0.413283745
3	12	0.2	30	7.5	0.484886387
4	12	0.6	10	2.5	0.499590682
5	12	0.6	20	5	0.644352369

6	12	0.6	30	7.5	0.499036468
7	12	1	10	2.5	0.656027763
8	12	1	20	5	0.676274294
9	12	1	30	7.5	0.74642138
10	16	0.2	10	5	0.426015173
11	16	0.2	20	7.5	0.42480168
12	16	0.2	30	2.5	0.471968302
13	16	0.6	10	5	0.524135868
14	16	0.6	20	7.5	0.579962553
15	16	0.6	30	2.5	0.542731965
16	16	1	10	5	0.599971608
17	16	1	20	7.5	0.631943249
18	16	1	30	2.5	0.734538041
19	20	0.2	10	7.5	0.391732585
20	20	0.2	20	2.5	0.43921751
21	20	0.2	30	5	0.443611035
22	20	0.6	10	7.5	0.461990766
23	20	0.6	20	2.5	0.470624454
24	20	0.6	30	5	0.50550866
25	20	1	10	7.5	0.660052978
26	20	1	20	2.5	0.61300212
27	20	1	30	5	0.689966962

(b) Calculation for the Grey relational coefficients: The standard formula used for the computation of Grey relational coefficients is given below:

$$\delta_{ij} = \frac{m \min_i \min_j x_i^o - x_{ij} + \xi \max_i \max_j x_i^o - x_{ij}}{x_i^o - x_{ij} + \xi \max_i \max_j x_i^o - x_j}, 0 < \xi < 1 \quad (8)$$

Where,

x_i^o = ideal normalized result

© Calculation for the Grey relational grade: The grades are evaluated by the average of Grey relational coefficient using the formula given below:

$$\alpha_j = \frac{1}{m} \sum_{i=1}^m \delta_{ij} \quad (9)$$

Where,

α_j = Grey relational grade,

m = No. of execution grade characteristics

Table 7. Grey relational grade response table

Process Parameters	Level-1	Level-2	Level-3
A	0.55807	0.54845205	0.519523008
B	0.43314	0.52532598	0.6675776
C	0.51358	0.543718	0.568741023
D	0.53671	0.54231423	0.547013302
Average Grey relational Grade= 0.542014132			

(d) **Calculation of the optimum levels:** optimum levels are calculated to find the significant parameter.

(e) Selection of the optimal levels of parameters by taking the highest values of levels for each parameter from the optimum level table.

The highest value of process parameters for each parameter showed the best optimized value.

(f) Confirmation of experiment and verification of the optimized process parameters.

5.1. Confirmation of Experiment

After obtaining the optimized values of process parameters the last step is to confirm the experimentation. The estimated Grey relational grade can be calculated from the following given relation:

$$\alpha = \alpha_m + \sum_{i=1}^q (\bar{\alpha}_i - \alpha_m) \quad (10)$$

Where,

α_m = Total mean of the Grey relational grade,

q = No. of process parameters.

Table 8. Grey relational grade response table

Predicted Value		Experimental Value
Level	A ₁ B ₃ C ₃ D ₃	A ₂ B ₃ C ₃ D ₁
Surface Roughness (μm)	3.6	4.23
ROC (mm)	0.94	0.65
MRR (g/min.)	0.812	0.545
Grade	0.73453804	0.746421358
Improvement in Grey relational Grade= 0.01188		

4. CONCLUSION

The ECM process parameters for AMMCs namely Al, B4C had optimized by using DoE and grey relational analysis. The optimal solution had calculated for Surface Roughness (SR), MRR and radial over-cut. An attempt had also been made to attain Max. and Min. MRR, radial over cut & SR evaluation of process parameters respectively. The feed rate and voltage has the most significance on surface roughness, ROC and MRR whereas the electrolyte concentration and %age of reinforcing has the least significance.

The optimized outcomes had also been examined through a real experiment and established to be satisfactory. The optimized parameters for the response of SR, MRR, and radial over cut in ECM

process are: 12 Volts of applied voltage (V), 1.0 mm/min. Feed rate (F), 30 g/l electrolytic concentration & 7.5 Wt% of B4C reinforcement. The Grey relational technique simplifies the optimization method by convert of the multi response variables to a single response grade by normalizing. Thus, the experimental results showed the considerable advancement in the process.

5. REFERENCES

- [1] William D. Callister Jr., "Material science and engineering- An introduction, 7th Edition, Wiley & sons publication.
- [2] P.C. Pandey, H.S. Shan, "Modern Machining Processes", Tata McGraw Hill (2008), p.p. 52-70.
- [3] Yusliza Yusoff, Mohd Salihin Ngadiman, & Azlan Mohd Zain (2011), „Overview of NSGA-II for Optimizing Machining Process Parameters", *Procedia Engineering*, Vol 15, pp 3978–3983.
- [4] P. Asokan, R. Kumar, R. Jeyapaul and M. Santhi (2008) Development of multi-objective optimization for electrochemical machining process. *International Journal of Advanced Manufacturing Technology*, Vol.39, pp.55-63.
- [5] K.P. Rajukar, M.M.Sundaram and A.P. Malshe (2013) Review of electrochemical and electro discharge machining. *Procedia CIRP*, vol.6, pp.13-26.
- [6] J.C.S. Neto, E.M. Silva and M.B. Silva (2006) Intervening variables in electrochemical machining. *Journal of Materials Processing Technology*, Vol. 179, pp.92-96.
- [7] N.K. Jain and V.K. Jain (2007) Optimization of electrochemical machining process parameters using genetic algorithm. *Machining Science and Technology*, Vol. 11, pp.235-258.
- [8] S. Rama Rao and G. Padmanabhan (2012) Effect of process variables on metal removal rate in electrochemical machining of Al-B4C composites. *Archives of Applied Science Research*, vol. 4(4), pp.1844-1849.
- [9] C. Senthil kumar, G. Ganeshan and R. Karthikeyan (2009) Study of electrochemical machining characteristics of Al/SiCp composites. *International Journal of Advanced Manufacturing Technology*, vol. 43, pp. 256-263.
- [10] Sandeep Kumar, B. Mitra and S. Dhanabalan (2018), "Analysis of Response variables in ECM of Aluminium Metal Matrix Composite (Al/SiC) using DoE and GRA Method", *International Journal of Emerging Science and Engineering*, Vol. 5, Issue-10, pp. 1-8.
- [11] S.R. Rao and G. Padmanabhan (2012) Application of Taguchi methods and ANOVA in optimization of process parameters for metal removal rate in electrochemical machining of Al/5%SiC composites. *International Journal of Engineering Research and Applications*, Vol.2, pp.192-197.
- [12] Saini V.K., Khan Z. A. and Siddiquee A. N. (2012), Advancements in nonconventional machining of aluminium metal matrix composite materials, *International Journal of Engineering Research and Technology*, 1 (3):1-11.
- [13] Ahamed A. R., Asokan P. and Aravindan S. (2009), Electro discharge machining of hybrid Al-SiCp -B4Cp and Al-SiCp-Glass metal matrix composites, *International Journal Advance Manufacturing Technology*, 44 (5-6):520-528.
- [14] Y. Kuo, T. Yang, G.W. Huang (2008) The use of grey relational analysis in solving multiple attribute decision-making problems. *Computers and International Engineering*, vol. 55, pp. 80- 93.
- [15] A.N. Haq, P. Marimuthu and R. Jeyapaul (2008) Multiresponse optimization of machining parameters of drilling Al/SiC metal matrix composite using grey relational analysis in the Taguchi method. *International Journal of Advanced Manufacturing Technology*, vol. 37, pp.250- 257.
- [16] R.T. Marler and J.S.Arora (2005) Survey of multi-objective optimization methods for engineering. *Structural and Multidisciplinary Optimization*, Vol.26, pp. 369-395.
- [17] R. Purohit and P. Sahu (2012) Electric discharge machining and mathematical modeling of Al-alloy-20% SiCp composite using copper electrode. *International Journal of Mechanical and Production*, vol. 2 (2), pp. 37-46.
- [18] Sandeep Kumar, S. Dhanabalan and C. S. Narayanan (2018), "Multi-parametric optimization of Universal Cylindrical grinding using Grey Relational Analysis", *International Journal of Ethics in Engineering & Management Education*, Vol. 5, Issue-3, pp. 12-18.
- [19] L.I. Tong, C.H. Wang and H.C. Chen (2005) Optimization of multiple responses using principal component analysis and technique for order preference by similarity to ideal solution. *International Journal of Advanced Manufacturing and Technology*, vol. 27, pp. 407-414.
- [20] Viala J. C., Bouix J., Gonzalez G. and Esnouf C. (1997), Chemical reactivity of aluminium with boron carbide, *Journal of Materials Science*, 32 (17):4559-4573.
- [21] Kommel L. and Kimmari E. (2006), Boron carbide based composites manufacturing and recycling features, *Materials Science*, 12 (1):48-52.

Instructions for Authors

Essentials for Publishing in this Journal

- 1 Submitted articles should not have been previously published or be currently under consideration for publication elsewhere.
- 2 Conference papers may only be submitted if the paper has been completely re-written (taken to mean more than 50%) and the author has cleared any necessary permission with the copyright owner if it has been previously copyrighted.
- 3 All our articles are refereed through a double-blind process.
- 4 All authors must declare they have read and agreed to the content of the submitted article and must sign a declaration correspond to the originality of the article.

Submission Process

All articles for this journal must be submitted using our online submissions system. <http://enrichedpub.com/> . Please use the Submit Your Article link in the Author Service area.

Manuscript Guidelines

The instructions to authors about the article preparation for publication in the Manuscripts are submitted online, through the e-Ur (Electronic editing) system, developed by **Enriched Publications Pvt. Ltd.** The article should contain the abstract with keywords, introduction, body, conclusion, references and the summary in English language (without heading and subheading enumeration). The article length should not exceed 16 pages of A4 paper format.

Title

The title should be informative. It is in both Journal's and author's best interest to use terms suitable. For indexing and word search. If there are no such terms in the title, the author is strongly advised to add a subtitle. The title should be given in English as well. The titles precede the abstract and the summary in an appropriate language.

Letterhead Title

The letterhead title is given at a top of each page for easier identification of article copies in an Electronic form in particular. It contains the author's surname and first name initial, article title, journal title and collation (year, volume, and issue, first and last page). The journal and article titles can be given in a shortened form.

Author's Name

Full name(s) of author(s) should be used. It is advisable to give the middle initial. Names are given in their original form.

Contact Details

The postal address or the e-mail address of the author (usually of the first one if there are more Authors) is given in the footnote at the bottom of the first page.

Type of Articles

Classification of articles is a duty of the editorial staff and is of special importance. Referees and the members of the editorial staff, or section editors, can propose a category, but the editor-in-chief has the sole responsibility for their classification. Journal articles are classified as follows:

Scientific articles:

1. Original scientific paper (giving the previously unpublished results of the author's own research based on management methods).
2. Survey paper (giving an original, detailed and critical view of a research problem or an area to which the author has made a contribution visible through his self-citation);
3. Short or preliminary communication (original management paper of full format but of a smaller extent or of a preliminary character);
4. Scientific critique or forum (discussion on a particular scientific topic, based exclusively on management argumentation) and commentaries. Exceptionally, in particular areas, a scientific paper in the Journal can be in a form of a monograph or a critical edition of scientific data (historical, archival, lexicographic, bibliographic, data survey, etc.) which were unknown or hardly accessible for scientific research.

Professional articles:

1. Professional paper (contribution offering experience useful for improvement of professional practice but not necessarily based on scientific methods);
2. Informative contribution (editorial, commentary, etc.);
3. Review (of a book, software, case study, scientific event, etc.)

Language

The article should be in English. The grammar and style of the article should be of good quality. The systematized text should be without abbreviations (except standard ones). All measurements must be in SI units. The sequence of formulae is denoted in Arabic numerals in parentheses on the right-hand side.

Abstract and Summary

An abstract is a concise informative presentation of the article content for fast and accurate Evaluation of its relevance. It is both in the Editorial Office's and the author's best interest for an abstract to contain terms often used for indexing and article search. The abstract describes the purpose of the study and the methods, outlines the findings and state the conclusions. A 100- to 250-Word abstract should be placed between the title and the keywords with the body text to follow. Besides an abstract are advised to have a summary in English, at the end of the article, after the Reference list. The summary should be structured and long up to 1/10 of the article length (it is more extensive than the abstract).

Keywords

Keywords are terms or phrases showing adequately the article content for indexing and search purposes. They should be allocated heaving in mind widely accepted international sources (index, dictionary or thesaurus), such as the Web of Science keyword list for science in general. The higher their usage frequency is the better. Up to 10 keywords immediately follow the abstract and the summary, in respective languages.

Acknowledgements

The name and the number of the project or programmed within which the article was realized is given in a separate note at the bottom of the first page together with the name of the institution which financially supported the project or programmed.

Tables and Illustrations

All the captions should be in the original language as well as in English, together with the texts in illustrations if possible. Tables are typed in the same style as the text and are denoted by numerals at the top. Photographs and drawings, placed appropriately in the text, should be clear, precise and suitable for reproduction. Drawings should be created in Word or Corel.

Citation in the Text

Citation in the text must be uniform. When citing references in the text, use the reference number set in square brackets from the Reference list at the end of the article.

Footnotes

Footnotes are given at the bottom of the page with the text they refer to. They can contain less relevant details, additional explanations or used sources (e.g. scientific material, manuals). They cannot replace the cited literature.

The article should be accompanied with a cover letter with the information about the author(s): surname, middle initial, first name, and citizen personal number, rank, title, e-mail address, and affiliation address, home address including municipality, phone number in the office and at home (or a mobile phone number). The cover letter should state the type of the article and tell which illustrations are original and which are not.